INHIBITION OF HIV-1 VIF BY POKEWEED ANTIVIRAL PROTEIN AND ITS IMPACT ON CELLULAR IMMUNE DEFENSE

GABRIELA KRIVDOVA

A THESIS SUBMITTED TO FACULTY OF GRADUATE STUDIES IN PARTIAL FULFILLMENT OF THE REQUIREMENTS FOR THE DEGREE OF

MASTER OF SCIENCE

GRADUATE PROGRAM IN BIOLOGY
YORK UNIVERSITY
TORONTO, ONTARIO
December 2014

ABSTRACT

Apolipoprotein B mRNA-editing enzyme, catalytic polypeptide-like editing complex 3G (APOBEC3G) is a DNA editing enzyme that deaminates deoxycytidines, converting them to deoxyuridines. APOBEC3G hypermutates human immunodeficiency virus type 1 (HIV-1) DNA during reverse transcription, resulting in the inhibition of viral propagation. The HIV-1 accessory protein named viral infectivity factor (Vif) counteracts the antiviral action of A3G by targeting it for degradation. The objective of this work is to evaluate whether the inhibitory effect of Vif on A3G can be diminished by pokeweed antiviral protein (PAP) and to determine the effect of PAP on HIV-1 infectivity and viral production. PAP is an N-glycosidase synthesized by the pokeweed plant, *Phytolacca americana*. It was previously shown that PAP exhibits antiviral activity against a broad range of plant and animal viruses, including HIV-1, at concentrations that are not toxic to the cells. In this study, I show that expression of PAP in cells reduced Vif protein accumulation by depurinating Vif open reading frame (ORF). Decreased Vif protein levels in the presence of PAP were correlated with increased A3G levels in HeLa cells stably expressing A3G. The antiviral enzyme reduced viral particle release by approximately 100-fold and the virions released from PAP expressing cells were 11-fold less infectious compared to virions released from PAPx expressing cells, an active site mutant lacking catalytic activity. The expression of PAP in producer HeLa-A3G cells reduced the levels of HIV-1 proviral DNA in target Jurkat cells. Downregulation of Vif by PAP and its effect on A3G is a novel finding, suggesting that PAP enhances the cellular innate immunity against HIV-1 by inhibiting Vif protein expression.

ACKNOWLEDGMENTS

First of all, I would like to express my appreciation and gratitude to my supervisor Dr. Kathi Hudak for accepting me and having me as a student in her laboratory for over 3 years. During this time, Kathi has taught me how to think critically, design experiments, interpret data, follow and optimize experimental designs. Her dedication to research and teaching and her positive attitude and encouragement have created a very pleasant laboratory experience. I would like to thank her for her patience and guidance through my degree and for helping me to pursue my goals.

Next, I would like to thank Dr. White for being my advisor and providing me with advice and feedback regarding my project. I would also like to thank Dr. Bayfield and Dr. Hood for being members of my examination committee and reading through my thesis.

The time in Dr. Hudak's lab has been full of great memories and I would like to thank all of the current and past members for the great moments we have shared. Special thanks to Kass Jobst, Kira Neller, Alex Klenov, Shira Elion Jourard, and Luca Spremulli for the support and friendship. I would like to acknowledge and thank previous members of the lab, Mez Kutky, Alice Zhabokritsky, Lydia Burns and Rajita Karran for mentoring me when I joined the lab and for creating a great team environment. In addition, I thank all the past and present members of Dr. White's lab for their assistance and help with my experiments.

Finally, I would like to thank my family and close friends for their support, patience and encouragement that guided me through my Masters degree.

TABLE OF CONTENTS

LIST OF TABLES

LIST OF FIGURES

LIST OF COMMON ABBREVIATIONS

AID: activation–induced cytidine deaminase
AIDS: acquired immunodeficiency syndrome
APOBEC: Apolipoprotein B messenger RNA (mRNA)-editing enzyme catalytic polypeptide-like editing complex
BMV: Brome mosaic virus
CA: capsid
CRS: cis-acting repressive sequence
CTL: cytotoxic T cell
DMEM: Dulbecco's modified eagle medium
DTT: dithiothreitol
ECL: enhanced chemiluminescence
EDTA: ethylenediaminetetraacetic acid
EF-2: elongation factor-2
ELISA: enzyme-linked immunosorbent assay
Env: envelope
ER: endoplasmic reticulum
ERK: extracellular signal-regulated kinase
FBS: fetal bovine serum
Gag: group-specific antigen
GALT: gut-associated lymphoid tissue
HA: hemagglutinin
HAART: highly active antiretroviral therapy
HBV: hepatitis virus B
HEK: human embryonic kidney
HPV: human papillomavirus
HSV: herpes simplex virus
HTLV: human T-cell leukemia virus
IN: integrase
LB: Luria-Bertani
LTNP: long-term non-progressor
LTR: long terminal repeat
MA: matrix
M-MuLV RT: Moloney-murine leukemia virus reverse transcriptase
NC: nucleocapsid
Nef: negative effector
ORF: open reading frame
PAP: pokeweed antiviral protein
PBMC: peripheral blood mononuclear cells
PBS: phosphate buffered saline
PCI: phenol:chloroform:isoamyl alcohol
PIC: preintegration complex
Pol: polymerase
PR: protease
PVX: potato virus X
qPCR: quantitative polymerase chain reaction

Rev: regulator of expression of virion proteins
RIP: ribosome inactivating protein
RNP: ribonucleoprotein
rRNA: ribosomal RNA
RT: reverse transcriptase
SDS-PAGE: sodium dodecyl sulfate-polyacrylamide gel electrophoresis
SOCS: suppressor of cytokine signalling
SU: surface protein
Tat: transactivator of transcription
TGF-β: transforming growth factor beta
TM: transmemrane
TMV: tobacco mosaic virus
Vif: viral infectivity factor
Vpr: virion protein R
Vpu: virion protein unique to HIV-1
VSV-G: vesicular stomatitis virus-glycoprotein G
ZDD: zinc-dependent deaminase domain

1. INTRODUCTION

1.1 APOBEC family of enzymes

1.1.1 General characteristics

Apolipoprotein B messenger RNA (mRNA)-editing enzyme catalytic polypeptide-like editing complex (APOBEC) family of proteins consists of 11 members in humans: activation-induced cytidine deaminase (AID), APOBEC1 (A1), APOBEC2 (A2), APOBEC3 (A3: A3A, A3B, A3C, A3DE, A3F, A3G, A3H), and APOBEC4 (A4). All members of APOBEC family of proteins act as cytidine deaminases, converting cytidines to uridines in RNA or deoxycytosines to deoxyuridines in single-stranded DNA (ssDNA) substrates (Pathak et al. 2014, Smith et al. 2012). This enzymatic activity is achieved with zinc-dependent cytidine or deoxycytidine deaminase domain (ZDD) organized as $HXEX_{23-28}$-$PCX_{2-4}C$, which allows the removal of exocyclic amine (Jarmuz et al. 2002, Wedekind et al. 2003). The zinc ion is coordinated by histidine and two cysteine residues located within ZDD (Smith et al. 2012). Glutamic acid is important for the deaminase activity by shuttling protons in the active site (Jarmuz et al. 2002). AID, A1, A3A, A3C and A3H contain one deaminase domain, while A3B, A3DE, A3F and A3G have two ZDDs (Wedekind et al. 2003, Smith et al. 2012, Jarmuz et al. 2002). Of the members with two ZDDs, the C-terminal ZDD has enzymatic activity, while the N-terminal Zn domain has high affinity for RNA-binding (Zheng et al. 2012). The second ZDD could have arisen by tandem duplication of the ancestral gene. Beside the conserved ZDD, all members share at least one active site cluster, a linker region and pseudoactive site domain (Hamilton et al. 2010). The schematic of APOBEC domain organization is illustrated in Figure 1.

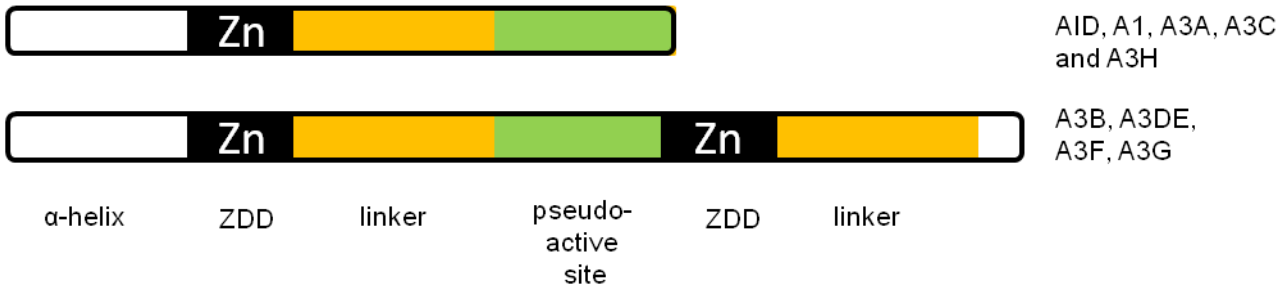

Figure 1. Schematic of APOBEC proteins' domain organization. All members of the family share conserved zinc deaminase domain (ZDD). While AID, A1, A3A, A3C and A3H contain one ZDD, A3B, A3DE, A3F and A3G have two ZDDs. The active site domain is joined by a linker to pseudo-active site.

1.1.2 Family members

A1 was the first mammalian cytidine deaminase identified as an enzyme that edits apolipoprotein B (apo B) pre-mRNA (Naratnam et al. 1993, Teng et al. 1993). Two versions of apoB proteins were found in human liver and intestine and this polymorphism was attributed to posttranscriptional RNA editing (Chen et al. 1987). Deamination of a specific cytidine (C6666) by A1 introduces a premature translation stop codon (UAA), resulting in a truncated apoB protein. This apoB protein variant plays an important role in lipid metabolism (Teng et al 1993, Navaratnam et al. 1993). The function of AID was discovered through subtractive hybridization screen that compared transcripts between resting and activated B cells undergoing immunoglobulin gene diversification (Muramatsu et al. 1999). AID is required for somatic hypermutation and class-switch recombination of immunoglubin genes and therefore antibody diversification (Muramatsu et al. 2000, Arakawa et al. 2002). A2 is expressed in skeletal and cardiac muscle where it was shown to play a role in muscle differentiation and maintenance of fiber-type ratios (Sato et al. 2010, Vonica et al. 2010, Etard et al. 2010). A2 also contributes to specification of left-right axis symmetry by regulating transforming growth factor β (TGFβ)

signalling during embryogenesis (Vonica et al. 2010). A4 is expressed in testes, but its function is unknown (Rogozin et al. 2005).

1.1.3 APOBEC3 enzymes

The discovery of APOBEC3 enzymes as inhibitors of retroviruses came from initially unrelated work in the field of HIV-1 studies. Research on HIV-1 revealed that mutants lacking a gene encoding the accessory protein viral infectivity factor (Vif) were unable to replicate in primary CD4+ T cells and macrophages, as well as some T-cell leukemia cell lines (e.g., CEM and H9 cells) (Gabuzda et al. 1992, Sakai et al. 1993). These cell lines were termed non-permissive since *vif*-deficient HIV-1 (HIV-1Δ*vif*) could not be propagated in them. In contrast, HIV-1Δ*vif* mutants were able to be propagated in permissive cell lines including all adherent cells (e.g., HEK293T and HeLa) and some T-cell lines (e.g., CEM-SS and SupT1). Fusion of non-permissive and permissive cells to create a heterokaryon revealed that the non-permissive phenotype was dominant (Simon et al. 1998). This suggested that a factor present in non-permissive cell lines was blocking replication of HIV-1Δ*vif*. cDNA subtraction between permissive and non-permissive cells identified APOBEC3G (A3G) as the restriction factor (Sheehy et al. 2002). Transfection of a construct encoding a functional A3G protein was sufficient to convert permissive phenotype to non-permissive (Sheehy et al. 2002). Therefore, A3G was identified as the factor that inhibits the propagation of HIV-1Δ*vif* in non-permissive cell lines.

Since the discovery of A3G as an HIV-1 restriction factor, A3 family of proteins has been intensely studied. The human A3 locus is located on chromosome 22 in humans (Jarmuz et al. 2002). While humans have 7 A3 genes, rodents, cats, pigs and sheep have only one A3 gene.

Two A3 genes are found in cows and 3 in dogs and horses (Smith et al. 2012). A3 proteins share approximately 50% sequence homology at the amino acid level (Cullen 2006). A3 enzymes are thought to function as components of innate immunity, to limit mobile genetic elements in the form of endogenous retroelements and exogenous viruses (Chiu et al. 2005, Peng et al. 2007, Koning et al. 2009, Reflsland et al. 2010, Esnault et al. 2006). Integration of retrotransposons may affect genetic stability by causing DNA deletions, insertions and rearrangements (Arias et al. 2012). Therefore, it is thought that A3 genes have expanded in primates to limit the retrotransposition of these mobile elements and infection of modern lentiviruses (Hamilton et al. 2010, Monameji et al. 2012). This is supported by the observed correlation between expansion of the A3 gene cluster and dramatic reduction in retrotransposition activity (Sawyer et al. 2004). Besides HIV-1, other exogenous viruses were shown to be targeted by A3 members, including human T cell leukemia virus type 1 (HTLV-1) (Sasada et al. 2005, Fan et al. 2010), hepatitis B virus (HBV) (Turelli et al. 2004), and human papillomavirus (HPV) (Vartanian et al. 2008). Therefore, A3 proteins can act as potent inhibitors of both, endogenous retroelements to protect genetic integrity, and exogenous viruses to enhance innate immunity.

Although A3G is the most well characterized member of the A3 family, other members, including A3F and A3DE have also been shown to target and inhibit the replication of HIV-1 and other retroviruses, although to a lesser extent (Bishop et al. 2004, Rose et al. 2005, Hulquist et al. 2011, Zielonka et al. 2009). Besides A3G, A3F is the second most potent suppressor of HIV-1 Vif. A3F recognizes different target sequence compared to A3G (Bishop et al. 2004, Liddament et al. 2004). Whereas A3G has a preference for dC<u>C</u> sequences, A3F preferentially deaminates T<u>C</u> targets (Liddament et al. 2004, Bishop et al. 2004).

1.2 APOBEC3G

1.2.1 A3G activity

A3G is the most well characterized and studied member of the APOBEC family due to its potent anti-HIV-1 activity. A3G is primarily expressed in CD4+ T lymphocytes and macrophages (Chiu et al. 2005, Peng et al. 2007, Koning et al. 2009, Reflsland et al. 2010). A3G is packaged into HIV-1Δ*vif* virions, which allows its close proximity to viral RNA and reverse transcription complex (Alce et al. 2004, Cen et al. 2004, Luo et al. 2004, Svarovskaia et al. 2004, Khan et al. 2004). After infection of susceptible cells, A3G mutates the viral genome during reverse transcription when the viral RNA is being transcribed into cDNA (Figure 2). A3G deaminates deoxycytosines into deoxyuridines in the minus-strand cDNA (Harris et al. 2003, Mangeat et al. 2003, Zhang et al. 2003). This editing activity of A3G is very efficient, resulting in up to 20% of all minus-strand dC residues being converted to dU residues (Cullen 2006). The editing occurs in graded frequency in the 5' to 3' direction across the HIV-1 genome; the regions of the genome that are reverse transcribed first are mutated the most (Yu et al. 2004). Since A3G targets ssDNA templates, it is the minus-strand DNA that gets edited because only the minus-strand proceeds through a transient single-stranded phase during reverse transcription. The graded frequency of deamination is caused by the differences in time that regions of the genome remain single-stranded (Yu et al. 2004a).

The introduction of deoxyuridines not normally found in DNA was hypothesized to attract DNA glycosylases and apurinic-apuyrimidinic endonucleases, resulting in degradation of viral cDNA (Schrofelbauer et al. 2005, Yang et al. 2007). Therefore, the observed decrease in the accumulation of viral reverse transcripts (Mariani et al. 2003, Mangeat et al. 2003, Iwatani et

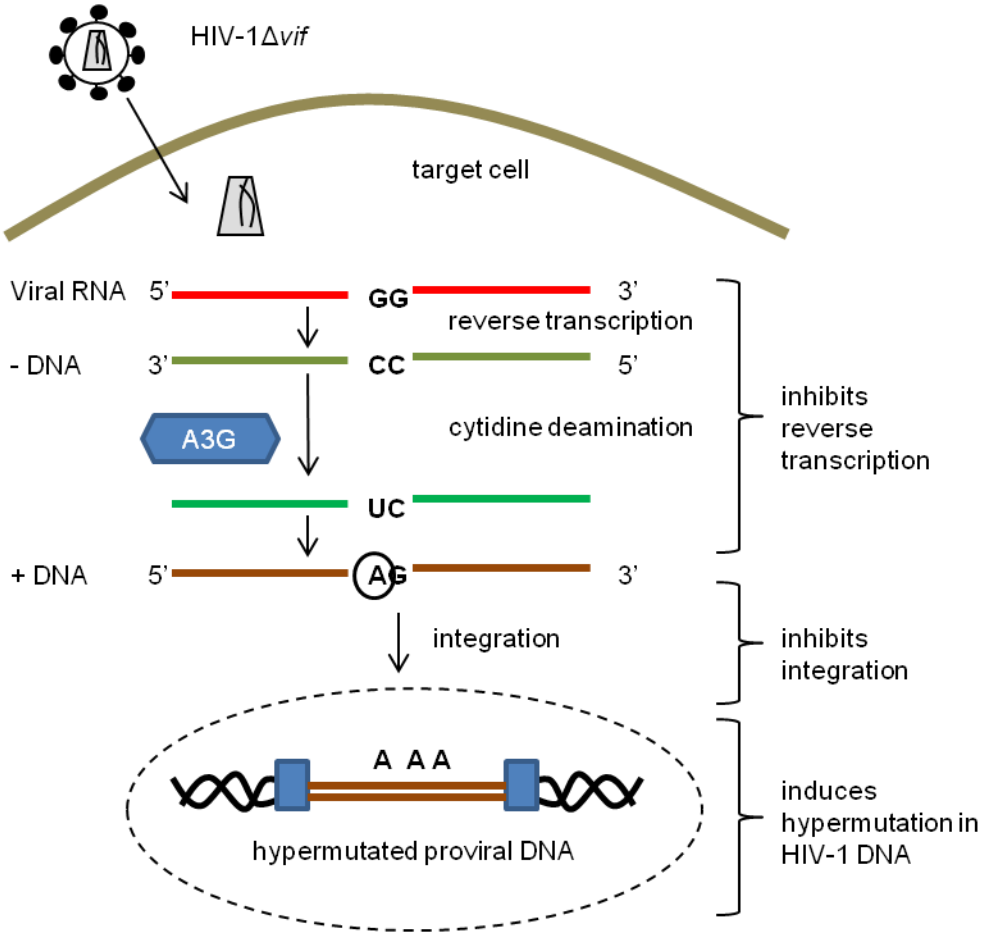

Figure 2. A3G restricts HIV-1Δ*vif* infection. Upon infection of a susceptible cell, A3G is released from *vif*-deficient HIV-1 virions. During reverse transcription of the HIV-1 RNA, A3G deaminates deoxycytosines in the minus-strand DNA, converting them into deoxyuracils. This in turn leads to deoxyguanine to deoxyadenine convertions in plus-strand DNA. Editing activity of A3G results in decreased reverse transcript accumulation and inhibition of proviral DNA integration. The integrated hypermutated HIV-1 DNA is largely defective due to introduction of premature stop codons and substitution mutations. Adapted from Desimmie et al. 2014.

al. 2007, Bishop et al. 2008) in the presence of A3G may be attributed to the action of DNA repair enzymes. However, this remains elusive as inhibition of uracil DNA glycosidases did not reverse A3G effect on HIV-1 cDNA levels (Langlois and Nauberger 2008).

Additionally, the editing activity of A3G causes deoxyguanine (dG) to deoxyadenosine (dA) conversions in the plus-strand cDNA, resulting in substitution mutations and premature translation stop codons that could cause a loss of genetic integrity (Harris et al. 2003, Mangeat et al. 2003, Yu et al. 2004, Zhang et al. 2003, Lecossier et al. 2003). A3G is also able to function through cytidine deamination-independent mechanisms by blocking different steps of reverse transcription, including annealing of the primer to viral RNA template, restricting DNA strand transfer, inhibiting elongation of reverse transcription and obstructing viral integration (Bishop et al. 2008, Newman et al. 2005, Mbisa et al. 2007, Li et al. 2007, Luo et al. 2007, Guo et al. 2007, Wang et al. 2012). The mechanism of HIV-1Δ*vif* restriction by A3G is illustrated in Figure 2.

1.2.2 Intravirion packaging of A3G

In the absence of Vif, A3G gets packaged into viral particles through its interaction with the nucleocapsid (NC) portion of the Gag polyprotein in RNA-dependent manner (Alce and Popik 2004, Cen et al. 2004, Khan et al. 2005, Luo et al. 2004, Schäfer et al. 2004, Svarovskaia et al. 2004, Zennou et al. 2004). The virion-packaged fraction of A3G is responsible for viral restriction in target cells and the number of A3G molecules packaged into virions depends on its cytosolic levels in the producer cell (Svarovskaia et al. 2004, Alce and Popik 2004, Xu et al. 2007). Virus particles released from peripheral blood mononuclear cells (PBMCs) were shown to contain approximately 3-11 molecules of A3G, which was effective for viral restriction (Xu et al. 2007). Using stochastic simulations and mathematical modelling, it was estimated that about

80% of progeny virions need to incorporate A3G in order to render HIV-1 infection unsustainable (Thangavelu et al. 2014). Therefore, the interplay between Vif and A3G modulates virus propagation. That is, high levels of A3G would increase viral DNA mutation load to significantly inhibit virus production, whereas low levels of A3G could potentially provide a selective advantage for the virus through non-lethal mutation rates that generate variants with increased fitness, such as drug resistance and the ability to escape from adaptive immune system (Simon et al. 2005, Sadler et al. 2010, Wood et al. 2009, Berkhout and deRonde 2004, Smith 2011). Therefore, complete inhibition of Vif activity might be required in order to prevent generation of virus variation and drug resistant strains arising from limited editing by A3G and must be considered in a design of new therapeutic approaches.

Some studies performed on HIV-1 infected patients showed inverse correlation between A3G expression levels and disease progression (Kourteva et al. 2012, Eyzaguirre et al. 2013, Ulenga et al. 2008, Jin et al. 2005). Long-term non-progressors (LTNPs) had higher A3G and A3F mRNA levels, lower virus burden and higher amount of hypermutated HIV-1 proviral DNA (Kourteva et al. 2012, Jin et al. 2005). Most of the defective HIV-1 genomes in LTNPs were caused by G to A hypermutation (Eyzaguirre et al. 2013). However, other studies showed no correlation between disease progression and A3G expression (Gandhi et al. 2008a). Thus, association between the ability to control viremia and A3G expression *in vivo* remains unclear.

1.3 Human Immunodeficiency virus type 1 (HIV-1)

1.3.1 General Characteristics

Human immunodeficiency virus type 1 (HIV-1) belongs to the *Lentivirus* genus of the *Retroviridae* family of viruses (Levy 1993). Retroviruses are enveloped viruses that contain virally encoded reverse transcriptase (RT) that converts the RNA genome into DNA during the process of reverse transcription. The members of the Lentivirus genus are associated with slow progression of disease (Levy 1993). HIV-1 was identified to be the causative agent of acquired immunodeficiency syndrome (AIDS) in 1983 by Luc Montagnier and Barre-Sinoussi (Barrè-Sinoussi et al. 1983). Since its discovery over 30 years ago, HIV-1 has infected over 60 million people and caused more than 25 million deaths (Merson et al. 2008). Therefore, HIV-1 has caused a major global pandemic, causing the highest mortality rates in developing countries including sub-Saharan Africa and South-East Asia.

HIV-1 is spread by sexual, percutaneous and intravenous routes, although 80% of all infections are sexually transmitted (Cohen et al. 2011). Once transmitted across the mucosal membrane, HIV-1 infects CD4+ T cells (helper T cells) and macrophages. The primary receptor is CD4 antigen present on the surface of both macrophages and CD4+ T cells. The virus also requires a co-receptor which is a chemokine receptor CCR5 or CXCR4 present on macrophages and T cells, respectively. During the acute infection, which occurs 4-6 weeks following the exposure to the virus, HIV-1 is rapidly expanded in gut-associated lymphoid tissue (GALT) and systematically, resulting in a sharp decline in helper T cells reservoirs (Cohen et al. 2011). The acute infection resolves and latency period of 8-10 years, characterized by clearance of the virus from circulation and replication in lymph nodes, follows (Cohen et al. 2011). During the latency period, there is a gradual depletion of CD4+ T cells which eventually results in acquired

immunodeficiency syndrome (AIDS). Patients suffer from wide range of opportunistic infections and malignancies such as sarcomas, lymphomas and neurological disorders due to compromised immune system (Levy 1993). The introduction of highly active antiretroviral therapy (HAART), which relies on a combination of drugs targeting different steps of viral replication, has dramatically improved the clinical outcome and life expectancy (Barrè-Sinousii et al. 2013). However, the drug therapy does not eradicate the virus and drug resistance, side effects and viral latency remain some of the difficulties associated with the present treatment (Barrè-Sinousii et al. 2013, Passaes and Sáez-Cirión 2014).

1.3.2 HIV-1 Structure and Genome Organization

HIV-1 is an enveloped virus with conical capsid enclosing 2 copies of the 9-kb RNA genome. Within the envelope, there are viral surface protein (SU, gp120) and transmembrane protein (TM, gp41) that are non-covalently attached. Matrix protein (MA, p17) lines the inner layer of the envelope. The conical capsid is made out of the virally encoded capsid protein (CA, p24). Inside the capsid, the viral RNA genome is coated with nucleocapsid (NC) protein. Virally encoded enzymes reverse transcriptase (RT), integrase (IN), and protease (PR) are present inside the virion. In addition, some accessory and regulatory proteins are packaged into the virion, including virion protein R (Vpr) and viral infectivity factor (Vif).

The HIV-1 genome is a plus-strand 9-kb RNA. Three genes common to all retroviruses are present: *gag* (group-specific antigen), *pol* (polymerases) and *env* (envelope proteins). *gag* encodes MA, NC and CA, *pol* encodes the viral enzymes PR, RT and IN and *env* encodes structural proteins SU and TM. In addition to the standard *gag*, *pol* and *env* genes, HIV-1 contains 6 additional open reading frames (ORFs) encoding regulatory proteins transactivator of

transcription (Tat) and regulator of expression of virion proteins (Rev) and accessory proteins negative effector (Nef), viral infectivity factor (Vif), virion protein R (Vpr) and virion protein unique to HIV-1 (Vpu). The schematic of HIV-1 genome organization is illustrated in Figure 3.

1.3.3 HIV-1 Life Cycle

HIV-1 infects CD4+ T cells and macrophages. SU (gp120) protein binds to CD4 receptor and CCR5 or CXCR4 co-receptor, which generates conformational changes that allow fusion of the viral envelope with the cell membrane (Stein 1987). Following the fusion, viral capsid is released into the cytosol and viral RNA is reverse transcribed by the RT enzyme to generate double-stranded proviral DNA. HIV-1 DNA along with IN and other proteins form a pre-integration complex (PIC) that allow translocation of the viral DNA into the nucleus (Arhel 2010). HIV-1 DNA is integrated into host chromosomal DNA by IN. Long terminal repeats (LTRs) are found on both ends of proviral DNA; 5' LTR serves as a promoter while 3' LTR plays a role in 3' processing of the viral RNA (Cullen 1991). Transcription from the 5' LTR generates full-length 9-kb RNA which encodes Gag and Gag/Pol polyproteins (Figure 3). The polyproteins are later processed by viral PR to generate the structural proteins and viral enzymes. Single splicing of the 9-kb transcript generates 4-kb class of RNAs from which Vif, Vpr, Vpu and Env are expressed. In addition, the RNAs can be further spliced to yield 2-kb class of RNAs that encode Tat, Rev and Nef (Levy 1993, Purcel and Martin 1993). Presence of multiple splice sites generates over 40 different mRNAs (Tazi et al. 2010).

Only the 2-kb class of RNAs can be transported out of the nucleus due to inhibitory cis-acting repressive sequences (CRS) present in 4-kb and 9-kb transcripts that are spliced out in 2-kb class of RNAs (Zhang et al. 1996). Therefore, the 9-kb and 4-kb RNAs are retained in the

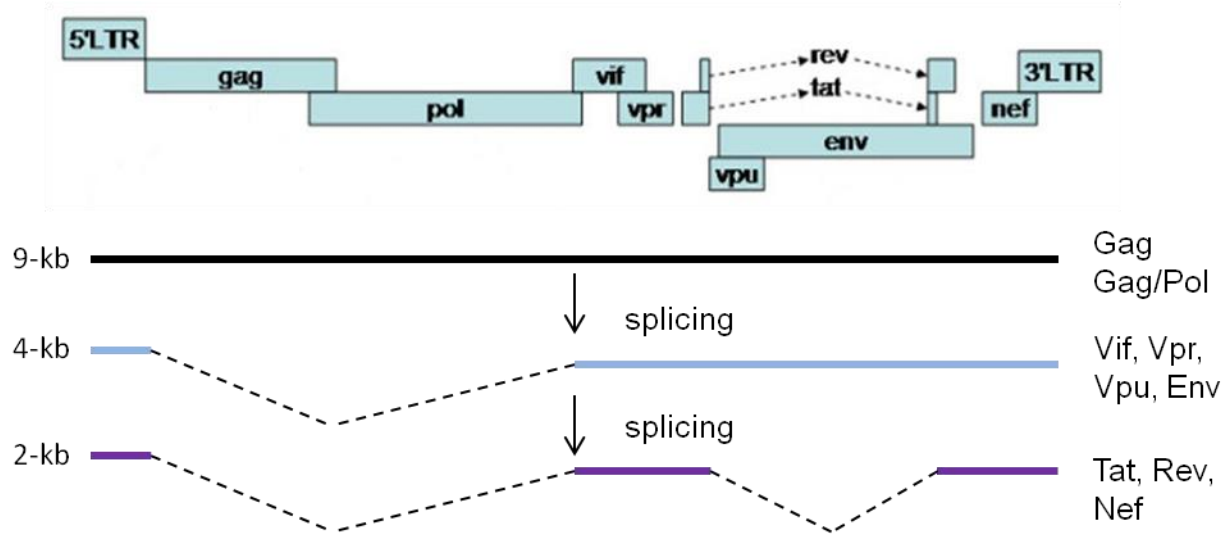

Figure 3. HIV-1 genome organization and processing. HIV-1 proviral DNA is transcribed to generate full-length 9-kb transcript from which Gag and Gag/Pol polyproteins are expressed. A single splicing event generates the 4-kb class of RNAs that encode Vif, Vpr, Vpu and Env. RNAs can be further spliced to make the 2-kb class of RNAs from which Tat, Rev and Nef are expressed.

nucleus until Rev is expressed, which then allows export of these transcripts into the cytosol (Pollard and Malim 1998). Viral RNAs are translated in the cytosol to generate the structural and regulatory proteins which then assemble to form new immature virus particles (Gottfredsson et al. 1997). These new virus particles bud off and proteolytic processing by PR allows their maturation and generation of infectious virions (Gottfredsson and Bohjanen 1997). The schematic of the HIV-1 life-cycle is shown in Figure 4.

1.4 Viral infectivity factor (Vif)

Vif is a 23 kDa protein encoded by the 4-kb class of HIV-1 RNAs. Vif's primary role is to target A3G for degradation and therefore counteract the antiviral activity of A3G. Vif interacts with E3 ubiquitin ligase complex consisting of Elongin B, Elongin C, Cullin 5 and Rbx 1 and hijacks it to mediate A3G polyubiquitination and subsequent degradation by the proteasome (Yu et al. 2003, Marin et al. 2003, Mehle et al. 2004, Sheehy et al. 2003, Stopak et al. 2003). In addition, the transcription factor CBF-β was shown to be recruited to this complex and be required for Vif-mediated degradation of A3G (Harris et al. 2011, Zhang et al. 2011). The amino acids residues required for the interaction between individual proteins and the assembly of the complex have been identified. The C-terminal of Vif contains a highly conserved suppressor of cytokine signalling (SOCS) motif which is required for the interaction with Elongin C (Yu et al. 2004b). Vif binds to Cullin 5 through a zinc-binding motif (Yu et al. 2004b). The interaction between Vif and A3G is species-specific and maps to a single amino acid D128 in A3G (Bogerd et al. 2004, Mangeat et al. 2004, Huthoff and Malim 2007). The schematic diagram of Vif interaction with A3G and the E3 ubiquitin ligase complex is shown in Figure 5.

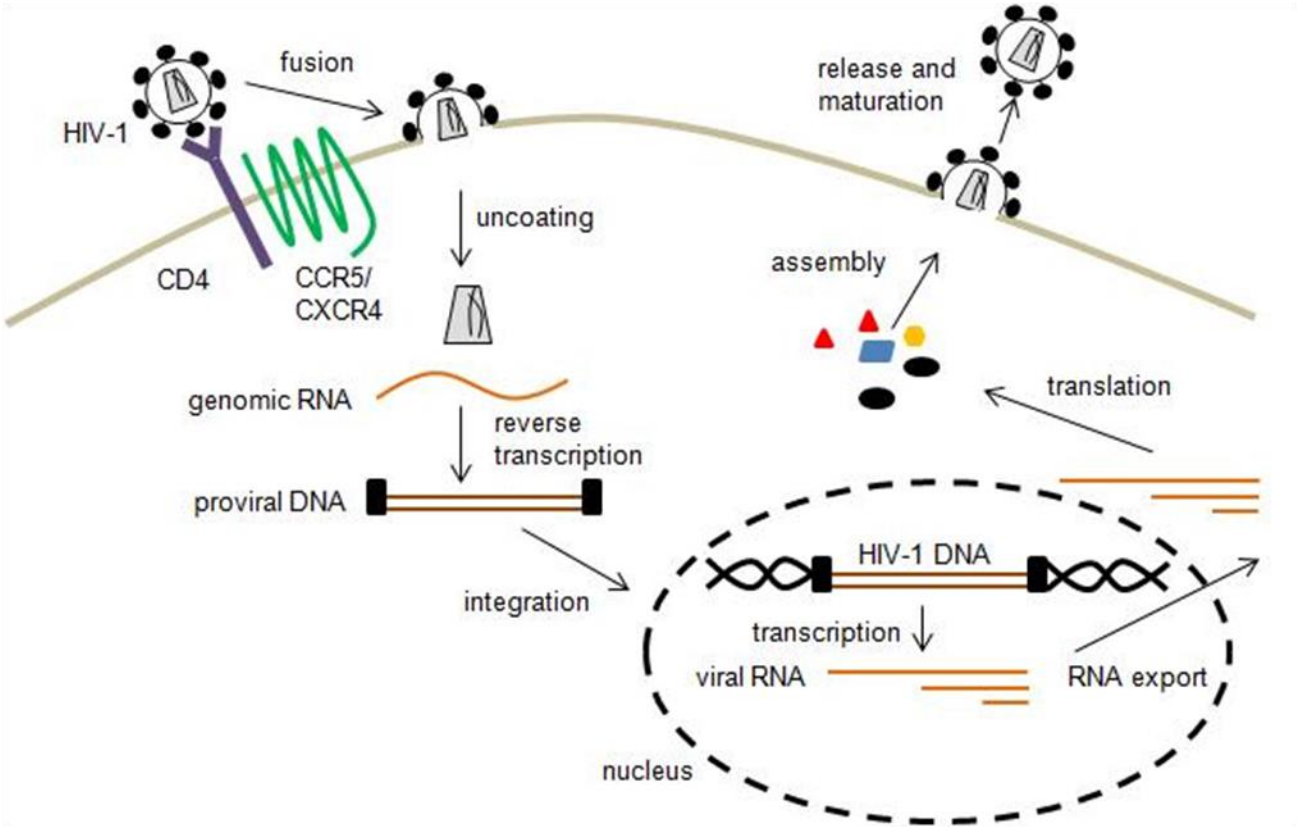

Figure 4. Schematic overview of the HIV-1 life cycle. HIV-1 binds to CD4 receptor and CCR5 or CXCR4 co-receptor. This induces fusion of the viral envelope with the cell membrane, resulting in the release of the capsid into the cytosol. The genomic RNA is reverse transcribed to produce proviral DNA, which is then integrated into host chromosomal DNA. Transcription generates viral RNAs that are exported out of the nucleus. Translation of viral RNAs produces structural and regulatory HIV-1 proteins. Assembly of viral particles occurs at the plasma membrane, after which the immature viral particles bud off. Viral particles mature after the release and form new infectious virions.

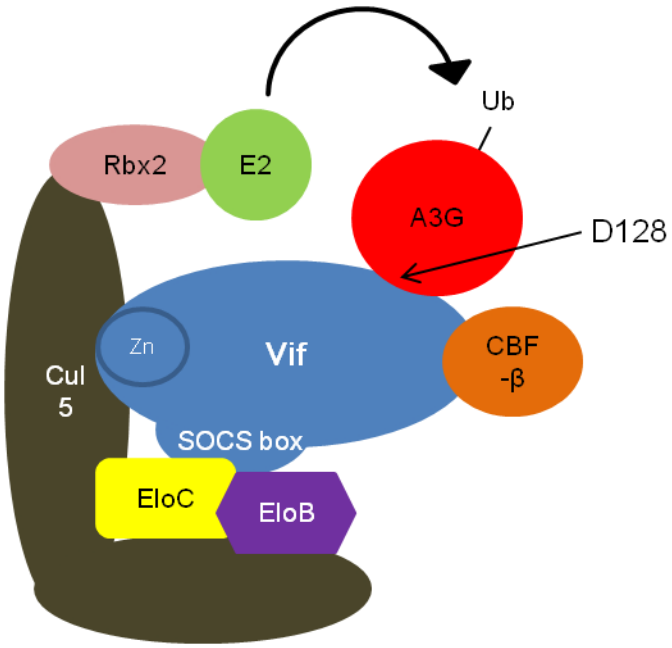

Figure 5. Interactions between Vif, A3G and the E3 ubiquitin ligase complex. Vif binds to Elongin C with the conserved SOCS motif, and to Cullin 5 with its zinc-binding motif. Association of Vif with E3 ubiquitin ligase allows ubiquitination of A3G. D128 residue in A3G is required for its association with Vif. Adapted from Malim and Beniasz 2012.

Therefore, in the presence of Vif, A3G is degraded, preventing its incorporation into nascent virions (Conticello et al. 2003, Kao et al. 2003, Marin et al. 2003, Sheehy et al. 2003, Stopak et al. 2003). In addition, Vif is able to prevent packaging of A3G into virions in a degradation-independent manner (Stopak et al. 2003, Mercenne et al. 2003, Opi et al. 2007, Kao et al. 2007, Kao et al. 2003). Inactive Vif variants were shown to reduce levels of A3G, suggesting that Vif may induce structural changes to prevent incorporation of A3G into virions or inhibit its enzymatic activity (Santa-Marta et al. 2005, Britan-Rosich et al. 2011). Overall, Vif counteracts the antiviral activity of A3G and therefore allows production of infectious viral particles.

1.5 Ribosome inactivating proteins (RIPs)

1.5.1 General characteristic of RIPs

Ribosome inactivating proteins (RIPs) are N-glycosidase enzymes ubiquitously expressed in different plants, fungi and bacteria (Girbes at al. 2004). These enzymes hydrolyze the N-glycosidic bond connecting the nitrogenous base to the ribose or deoxyribose in RNA or DNA substrates. The enzymatic action of RIPs as glycosidases depurinating ribosomal RNA (rRNA) was demonstrated in 1987 (Endo et al. 1987). RIPs depurinate a specific adenine (A4324) found within the highly conserved α-sarcin/ricin loop of the 28S rRNA, resuling in the inactivation of the ribosome (Endo et al. 1987) (Figure 6A). Depurination of rRNA inhibits the binding of elongation factor 2 (EF2), and therefore prevents the GTP-dependent translocation step of translation elongation mediated by EF2 (Montanaro et al. 1975, Gessner and Irvin 1980). As a consequence of the translation elongation arrest, the ribosome stalls at the point of the depurinated base (Gandhi et al. 2008b). Inhibition of protein translation is the cause of the observed toxicity of RIPs in cells (Gessner and Irvin 1980, Nilsson and Nygard 1986).

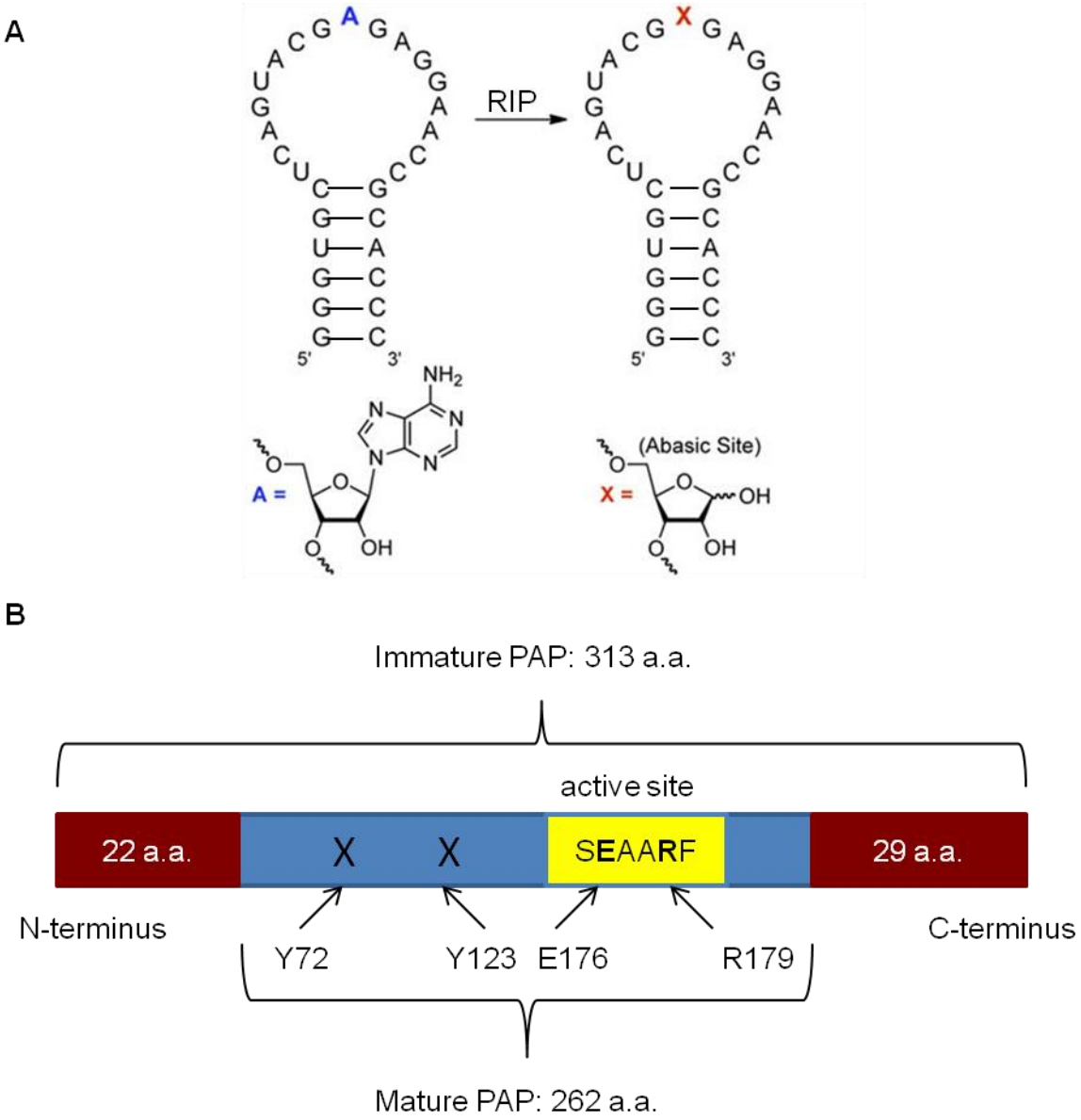

Figure 6. Schematic diagram of RIP N-glycosidase activity and PAP domain organization. **(A)** RIPs depurinate a specific adenine residue (A4324) located within the highly conserved α-sarcin/ricin loop of the 28S rRNA, leaving an abasic site. Adapted from Tor and Xie 2009. (B) Immature PAP is proteolytically processed by removing 22 amino acids (a.a.) from the N-terminus and 29 a.a. from the C-terminus to generate 262 a.a. mature PAP. Highly conserved SEAARF motif containing E176 and R179 residues that are directly involved in catalysis is located within the active site. Two tyrosine residues (Y72 and Y123) help to hold purine in the active site.

1.5.2 Classification

RIPs are classified into 3 major groups, Type I, II and III, based on their physical properties (Nielsen and Boston 2011). Type I RIPs contain a single polypeptide chain (A chain) of approximately 30-kDa (Nielsen and Boston 2001). Examples of Type 1 RIPs include pokeweed antiviral protein (PAP) from *Phytolacca*, saporin from *Saponaria* and trichosanthin from *Tricosanthes* (Stirpe 2004, Nielsen and Boston 2001). Type II RIPs consists of an enzymatically active A chain linked to lectin binding B chain via a disulfide bond (Stirpe 2004, Nielsen and Boston 2001). These heterodimeric Type II RIPs are toxic due to the ability of the lectin chain to bind sugars with galactose structure present on glycoproteins and glycolipids found on the surface of cell membranes (Nielsen and Boston 2001). This allows their endocytosis and translocation into the cytosol (Sandvig and van Deurs 1996). Ricin and abrin are examples of toxins that belong to this group (Stirpe et al. 2004). Type III RIPs are synthesized as inactive precursors and require proteolytic processing for activation (Nielsen and Boston 2001). Members of this group include JIP60 found in barley and b-32 RIP from maize (Stirpe 2004, Peumans et al. 2001).

1.5.3 Antiviral activity of RIPs

It is believed that RIPs play a role in defense against pathogens, such as viruses and fungi, and can also be involved in stress and senescense responses (Nielsen and Boston 2001). The antiviral activity of RIPs against different plant and animal viruses has been characterized, although the mechanism is poorly understood (Foà-Tomasi et al. 1982). In plants, RIPs are segregated away from ribosomes in cell wall matrix or vacuoles and it is thought that infection of a plant with a virus allows the release of the RIP from its sub-cellular compartment into the

cytosol and subsequent cell death due to translational inhibition (Nielsen and Boston 2001, Stirpe 2004). However, the observed inhibition of viral replication in absence of translational inhibition suggest that antiviral activity of some RIPs can be dissociated from their ability to depurinate rRNA (Tumer et al. 1997, Teltow et al. 1983, Huang et al. 1999, Mansouri et al. 2009). In addition, some RIPs were shown to directly depurinate viral RNAs, including human immunodeficiency virus type 1 (HIV-1), human T-cell leukemia virus 1 (HTLV-1) and brome mosaic virus (BMV) (Rajamohan et al. 1999, Mansouri et al. 2009, Gandhi et al. 2008b). The lack of cytotoxicity associated with expression of RIPs in cells contradicts the translational inhibition observed when higher concentrations of RIPs were used. Therefore, at low concentrations, some RIPs may inhibit viral replication without causing significant cytotoxicity, which makes them interesting candidates for biotherapeutic agents against virus infections.

1.6 Pokeweed antiviral protein (PAP)

1.6.1 General Characteristics

Pokeweed antiviral protein (PAP) is a Type 1 RIP synthesized by the pokeweed plant, *Phytolacca americana.* In pokeweed, PAP is synthesized as a precursor and undergoes proteolytic processing in endoplasmic reticulum (ER). The immature 313 amino acid precursor is processed by cleaving 22 amino acid N-terminal signal peptide and 29 amino acid C-terminal extension to yield the mature protein (Hur et al. 1995). The mature PAP is targeted into the cell wall, thereby segregating it away from ribosomes and preventing its cytotoxic effects (Ready et al. 1986). PAP contains a highly conserved SEAARF motif (amino acids 175-180), which contains the residues involved in catalysis (Monzingo et al. 1993). Glutamate 176 (E176) is located within the active site and its mutation to valine (E176V) renders the protein catalytically

inactive (Hur et al. 1995). Arginine 179 (R179) is also universally conserved and involved in catalysis (Monzingo et al. 1993). The crystal structure of PAP shows that two tyrosine residues (Y72 and Y179) help to coordinate the purine in the active site (Monzingo et al. 1993). Mutational studies revealed that an intact C-terminus was required for toxicity and depurination of ribosomes *in vivo* (Tumer et al. 1997). A schematic diagram of PAP structure organization and its important residues are illustrated in Figure 6B.

1.6.2 Antiviral Activity of PAP

The antiviral activity of PAP was first documented when crude extracts from pokeweed leaves were shown to inhibit Tobacco mosaic virus (TMV) infection when they were mixed and applied to plant leaves (Duggard and Armstrong 1925). Since then, antiviral activity of PAP against many plant and animal viruses, including brome mosaic virus (BMV), herpes simplex virus-1 (HSV-1), human T-cell leukemia virus 1 (HTLV-1) and human immunodeficiency virus type 1 (HIV-1), was reported (Teltow et al. 1983, Aaron and Irvin 1980, Zarling et al. 1990, Rajamohan et al. 1999, Mansouri et al. 2009, Karran and Hudak 2008). PAP inhibited HSV-1 replication in HeLa and Vero cells at concentrations that were not toxic to the cells (Aaron and Irvin 1980). Similarly, inhibition of HTLV-1 replication when PAP was expressed in HEK293T cells was not associated with decreased viability (Mansouri et al. 2009). The independence of antiviral activity and depurination of ribosomes was further supported when C-terminal mutant of PAP was shown to inhibit replication of potato virus X (PVX) while being unable to depurinate ribosomes (Tumer et al. 1997). These studies showed that the antiviral activity of PAP might be separable from its rRNA depurination ability, suggesting that there is an alternative mechanism of limiting virus replication. It is unclear how PAP could preferentially

target viral RNAs for depurination, secondary structure or localization of viral RNAs could play a role, but further studies are needed to investigate this topic.

1.6.3 Antiviral activity of PAP against HIV and its application

By monitoring adenine release, PAP was shown to depurinate HIV-1 RNAs in concentration dependent matter (Rajamohan et al. 1999). Further studies showed that purified PAP inhibited HIV-1 production in primary human CD4+ T cells (Zarling et al. 1990). Conjugation of PAP to antibodies directed against antigens present of CD4+ T cells forms immunotoxins with increased delivery of PAP into plasma membrane. PAP immunoconjugates containing antibodies against CD4, CD5 or CD7 antigens present on helper T cells resulted in the inhibition of HIV-1 replication at picomolar concentrations of the immunotoxin used and increased the anti-HIV activity by 1000-fold (Zarling et al. 1990). Also, the immunoconjugates showed a longer plasma half-life compared to free PAP (Zarling et al. 1990). In a separate study, an immunoconjugate made up of PAP and anti-CD4 antibody inhibited replication of 22 clinical HIV-1 strains at concentrations that did not affect proliferation of CD4+ T cells (Erice et al. 1993). Administration of an immunotoxin TXU-PAP composed of purified PAP and anti-CD7 antibody to HIV-1 infected chimpanzees and adult patients decreased HIV-1 RNA levels but no sustained therapeutic effect was observed at the concentration tested (Uckun et al. 1999). Some complications associated with PAP immunoconjugates included side-effects, such as elevation of liver enzymes, short plasma half-life, and generation of antibodies directed against the immunotoxin (Uckun et al. 1999). A better understanding of the mechanism of PAP antiviral activity could help in a design of therapeutic agents or imunotoxins with more desirable characteristics.

1.7 Project Goals

Previous studies conducted in our lab and elsewhere showed that PAP depurinates HIV-1 RNAs (Rajamohan et al. 1999, Zhabokristky et al. 2014). Recently, it was shown that PAP depurinates Rev RNA, resulting in altered ratio of HIV-1 RNAs (Zhabokritsky et al. 2014). The absence of functional Rev protein caused retention of 9-kb and 4-kb RNAs in the nucleus and increased their availability for splicing. However, despite the recovery of the splicing ratio when Rev was overexpressed in the presence of PAP, the viral protein expression was not rescued (Zhabokritsky et al. 2014). Therefore, even if HIV-1 RNAs are exported to the cytosol, they are most likely targets for depurination, which results in the inhibition of expression of functional viral proteins. In my project, I wanted to investigate if PAP targets Vif mRNA and its impact on Vif protein expression and immunity of cells against HIV-1.

Since Vif plays a role in infectivity of HIV-1 by counteracting the effect of the host restriction factor A3G, I wanted to determine the effect of PAP expression on the infectivity of HIV-1 produced in a cell line stably expressing A3G. Previous studies showed that transient expression of PAP inhibited HIV-1 production in HEK293T cells by approximately 450-fold (Mansouri et al. 2012). However, PAP increased the infectivity of the released viral particles by 7-fold (Mansouri et al. 2012). This increase in infectivity was attributed to activation of extracellular signal-regulated kinase 1/2 (ERK1/2) mitogen activated protein kinase (MAPK) pathway and subsequent phosphorylation of p17 matrix protein (Mansouri et al. 2012). This cell line does not express A3G, which is expressed endogenously in CD4+ T cells and macrophages, the natural targets of HIV-1.

Therefore, my project focused on determining the effect of PAP on Vif expression and its impact on the immune response mediated by A3G. **I hypothesized that targeting of Vif by PAP and the subsequent inhibition of protein expression would lead to elevated A3G levels and cause reduced infectivity of HIV-1 particles.** To investigate this, I used HEK293 and HeLa cells stably expressing A3G to study the effect of PAP on Vif and A3G protein levels. In addition, I used the HIV-1 indicator cell line 1G5 to determine the infectivity of HIV-1 virions released from PAP expressing cells and the levels of HIV-1 DNA integration.

2. MATERIALS AND METHODS

2.1 Cell culture

Human embryonic kidney (HEK) 293T cells were maintained in Dulbecco's Modified Eagle Medium (DMEM) (Life Technologies) supplemented with 10% fetal bovine serum (FBS) (Life Technologies) and penicillin (100 U/ml) and streptomycin (100 μg/ml) at pH 7.4. HEK293-A3G and HeLa-A3G cells (NIH AIDS Reference and Reagent Program, catalog ue #10203 and #9907, respectively) contain stably integrated A3G gene. Cell lines were cultured in DMEM supplemented with 10% FBS and G418 disulfate salt (100 μg/ml) (Sigma) at pH 7.4. Cells were maintained under G418 selection for passaging, but the antibiotic was removed from media for experiments. Cells were grown in polysterene treated plates in a humidified incubator (Thermo Electron Corporation HEPA Class 100) at 37°C and 5% CO_2. Cells were passaged at 1:5 split every second day. Washing of the cells was done with 1X phosphate buffered saline (PBS) (135 mM NaCl, 5 mM Na_2HPO_4, 2.5 mM KCl, 2 mM KH_2PO_4 pH 7.4). Following the wash, 1 ml of 0.25% Trypsin, 0.1% EDTA was added to allow detachment of the cells.

H9 lymphocytes (NIH AIDS Reference and Reagent Program, catalogue #87) were cultured in RPMI-1640 (Life Technologies) supplemented with 10% FBS and G418 (50 μg/ml). The HIV indicator cell line 1G5 (NIH AIDS Reference and Reagent Program, catalog # 1819) is a derivative of Jurkat cell line containing a stably integrated construct consisting of HIV-1 long terminal repeat (LTR) upstream of the Luciferase reporter gene. Cells were maintained in RPMI-1640 supplemented with 10% FBS, penicillin (100 U/ml) and streptomycin (100 μg/ml). Both lymphocytic cell lines were maintained at 1 x 10^5- 1.0 x 10^6 cells/ml by splitting the cells 1:5 every second day. Cells were grown in non-treated plates in a humidified incubator at 37°C and 5% CO_2.

2.2 Plasmid transfection and cell harvesting

2.2.1 Plasmid transfection

For adherent cell lines, cells were plated 18-24 hours prior to transfection to achieve optimal 70-80% confluency at the time of transfection. HEK293T cells were transfected using calcium phosphate precipitation method. Cells were re-fed with 10 ml of fresh growth medium 3 hours prior to transfection. Briefly, total plasmid DNA (20-25 μg) was diluted in 405 μl of dH_2O in 1.5 ml microtube and 45 μl of $CaCl_2$ was added by pipetting. The DNA containing mixture was then titrated into 15 ml tubes containing 450 μl of 2X HeBS buffer (350 mM NaCl, 60 mM Hepes pH 7.15, 1 mM Na_2HPO_4) with continuous slow vortexing. Samples were incubated for 20 minutes at room temperature to allow formation of DNA precipitates, after which they were added drop-wise onto plated cells. Transfection efficiency was determined by yellow fluorescent protein (YFP) expression using inverted fluorescent microscope (Axiovert) approximately 20 hours post transfection. Cells were washed with 5 ml of 1X PBS, re-fed with fresh medium and incubated for another 24 hours prior to harvesting.

For HEK293-A3G and HeLa-A3G cells, transfection was performed using Lipofectamine2000 reagent (Invitrogen). Cells were seeded in 6-well plates with antibiotic free medium to achieve 70-80% confluency at the time of transfection. Plasmid DNA (5-7 μg) was diluted in 50 μl of serum-free DMEM. Lipofectamine reagent (8-10 μl) was diluted in 50 μl of serum-free DMEM in a separate 1.5 ml microtube and incubated for 5 minutes at room temperature. After, diluted DNA was transferred to diluted lipofectamine and mixed gently by pipetting. The sample was incubated for 15-20 minutes at room temperature, after which the DNA-reagent complex was added drop-wise onto seeded cells. Cells were washed with 1 ml of 1X PBS and re-fed with 2 ml of fresh media 20 hours post transfection.

H9 lymphocytes were transfected using Lipofectamine2000 reagent. Cells (1.0×10^6) were resuspended in 3 ml antibiotic-free media in 6-well non-treated plates. Transfection with lipofectamine reagent was performed as described above. Transfection efficiency was estimated using YFP expression 20 hours post transfection and cells were harvested 20-24 hours later.

2.2.2 Harvesting

Harvesting of transfected adherent cells was performed 44-48 hours post transfection. Cells were washed with 1X PBS and resuspended in 1 ml of cold 1X PBS. To pellet the cells, samples were centrifuged at 9,000 x g for 5 minutes at 4°C. The supernatants were aspirated and the pellets were used for RNA or protein extraction. For harvesting of H9 and 1G5 cells, cells were centrifuged at 200 x g for 7 minutes, and washed with 1X PBS. Supernatants were aspirated and remaining pellets were used for RNA isolation.

2.3 MTT conversion assay

HeLa-A3G cells were seeded in 6-well plates to achieve 70-80% confluency at the time of transfection. Cells were transfected with pcPAP (0.25 - 1.0 μg), pcPAPx (1.0 μg) or pcDNA3 (1.0 μg) using Lipofectamine2000 as described above. On the following day, cells were washed with 1 ml of 1X PBS and 2 ml of fresh media was added. Cells were washed again and detached from the plate 48 hours post-transfection using trypsin solution and resuspended in 1 ml of fresh media. Next, 100 μl of resuspended cells were combined with 10 μl of MTT labelling reagent (Sigma-Aldrich) in a 96-well plate and incubated for 4 hours at 37°C. Following the incubation, 100 μl of solubilization buffer (Sigma-Aldrich) was added to each well. The plate was placed back into the incubator for additional 2 hours after which the absorbance of the samples was

measured at 595 nm wavelength using an ELISA plate reader (Beckman Coulter DTX880 Multimode Detector). Triplicates for each sample were performed. Values were presented as ratios relative to absorbance values obtained from samples transfected with pcDNA3 and represent means ± S.E. of three independent experiments.

2.4 RNA isolation

Cell pellets were lysed with 2 volumes of cytoplasmic lysis buffer (25 mM Hepes, pH 7.5, 2 mM EGTA, 1 mM DTT, 10% glycerol, 1% NP-40). Samples were vortexed, placed on ice for 10 minutes, and centrifuged at 14,000 x g for 10 minutes at 4°C to pellet cell debris. Supernatants were transferred to new 1.5 ml microtubes and 0.5 ml of Trizol (Molecular Research Center) and 100 µl of chloroform were added. Samples were vortexed, incubated at room temperature for 5 minutes and centrifuged at 16,000 x g for 10 minutes at 4˚C. Top, RNA-containing aqueous layer was transferred to new 1.5 ml microtubes and 0.5 ml of isopropanol and 10 µg of glycogen was added. RNA was precipitated at -20°C for 18 hours, followed by centrifugation at 16,000 x g for 30 minutes at 4°C. Pellets were air-dried and resuspended in 150 µl of dH_20. Next, 150 µl of phenol:chloroform:isoamyl alcohol (PCI) (25:24:1) was added, samples were vortexed and centrifuged at 16,000 x g for 5 minutes at room temperature. The top layer was extracted and 2.5 volumes of 100% ethanol and 1/10 volume of 3M NaOAc were added. RNA was precipitated at -20°C for 18 hours, followed by centrifugation at 16,000 x g for 30 minutes at 4°C. The supernatant was discarded and the pellet was washed with 70% ethanol by centrifuging the samples at 16,000 x g for 15 minutes at 4°C. Pellets were air-dried and resuspended in 15-30 µl of dH_2O. RNA was quantified using spectrophotometer (Beckman DU530 Life Sciences) at OD_{260} nm.

2.5 RNA Immunoprecipitation

To determine whether PAP associated with Vif RNA *in vivo*, immunoprecipitation of PAP-bound RNAs was performed. Cells were transfected with constructs encoding codon optimized Vif (pc-hVif) and PAP and the media was aspirated 48 hours post transfection, followed by washing of the cells with 5 ml of 1X PBS. After the wash, 7 ml of cold 1X PBS was added to the cells and RNA was crosslinked to proteins by irradiating the cells at 260 nm at 150 mJ/cm^2 for 10 minutes. After the generation of RNA-protein crosslinks, the cells were harvested by resuspending them in the 1X PBS and centrifuged at 4,000 x g for 5 minutes. The supernatant was aspirated and the resulting pellets were lysed with 2 volumes of cytoplasmic lysis buffer (25 mM Hepes, pH 7.5, 2 mM EGTA, 1 mM DTT, 10% glycerol, 1% NP-40). Samples were vortexed and placed on ice for 10 minutes, and centrifuged at 14,000 x g for 10 minutes at 4°C to pellet cell debris. Cell lysates were transferred to new 1.5 ml microtubes.

Goat anti-rabbit IgG magnetic beads (New England Biolabs) were resuspended in the supplied buffer by vortexing and rotating for 1.5 hours at 4˚C. After, 15 µl of resuspended beads was aliquoted to 1.5 microtubes and washed 3 times with 1X ribonucleoprotein (RNP) buffer (150 mM NaCl, 20 mM Hepes pH 7.4, 0.5% Triton X, 0.1% Tween 20, 8 units of RNase OUT) by adding 1 ml of the buffer, exposing the beads to a magnet (Dynal) and drawing them to the side to allow removal of the supernatant. Washed beads were resuspended in 200 µl of 1X PBS and incubated with 5-10 µg of rabbit polyclonal PAP antibody by rotating the 1.5 ml microtubes for 2 hours at 4˚C. Polyclonal PAP antibody-coated beads were then washed 3 times with 1X RNP buffer and cell lysates were added after the removal of the supernatant. Cell lysates were incubated with the coated beads by rotating the samples for 30 minutes at 4˚C. Samples were then washed 4 times with 1X RNP buffer and finally resuspended in 500 µl of 1X RNP buffer.

Proteins were digested by incubating the samples with 1% SDS and 3 units of proteinase K (BioShop) for 30 minutes at 30˚C. Following the incubation, proteins were removed by adding 500 µl of phenol:chloroform:isoamyl alcohol (PCI) (25:24:1). Samples were mixed by vortexing, centrifuged at 16,000 x g for 5 minutes at room temperature and the top layer was extracted. RNA was precipitated with 900 µl of 100% ethanol and 10 µg of glycogen at -20˚C overnight followed by centrifugation at 16,000 x g for 30 minutes at 4˚C. Supernatant was discarded and the pellet was washed with 500 µl of 70% ethanol by centrifuging the sample at 16,000 x g for 15 minutes at 4˚C. After air-drying the pellet for 5 minutes, the RNA was resuspended in 10 µl of dH_2O. The resuspended RNA was then used in RT-qPCR analysis to quantify levels of Vif RNA.

2.6 Reverse transcription (RT)

For the reverse transcription reaction, 10 µl of resuspended RNA obtained from RNA immunoprecipitation or 1-3 µg of cytosolic RNA harvested from transfected cells was used in a total volume of 10 µl. Appropriate reverse primer (0.2 µg) was added and samples were denatured at 95˚C for 3 minutes. Sequences of all primers used are listed in Table 1. Following the heating, samples were placed on ice for 1 minute and 2 µl of 5X first-strand buffer (375 mM KCl, 250 mM Tris-HCl pH 8.3, 15 mM $MgCl_2$, 5 mM DTT) was added. Primer was allowed to anneal by incubating the sample for 10 minutes at room temperature. After the incubation, 2 µl of first-strand buffer, 2 µl of 0.1 M DTT, 2 µl of 10 mM dNTPs, 2 µl of dH_2O, 40 units of RNase inhibitor (New England Biolabs) and 20 units of Moloney-murine leukemia virus reverse transcriptase (M-MuLV RT) (New England Biolabs) were added to each reaction. Samples were

Table 1. List of primers used in this study. The names of primers along with their sequences and melting temperatures are listed below.

Primer name	Sequence (5' - 3')	TM (°C)
hVif 431 F	CTCTACAGTACTTGGCACTAGCAGC	64.3
hVif 679 R	CTAGTGTCCATTCATTGTATG	58.4
HXB2 5200 F	CCTCATCCAAGAATAAGTTCAG	59.3
HXB2 5350 R	CTGCTAGTTCAGGGTCTACT	55.2
hVif 173 F	GATTAGCAGCGAGGTGCACATTCC	71.4
hVif 383 R	ATACGTCCTAATATGGTATTTC	59.9
HXB2 5460 R	GGTGTGAATATCAAGCAGGACATAAC	65.3
5S rRNA 24 F	GGGCCGGATCCCATCAGAACTCC	77.8
5S rRNA 96 R	CCCAGGAGGTCACCCA	69.8
28S rRNA dep R	AGTCATAATCCCACAGATGGT	53.4
28S rRNA R	TTCACTCGCCGTTACTGAGG	57.2

incubated for 90 minutes at 48˚C, followed by heat-inactivation of the enzyme at 70˚C for 10 minutes. Heat-inactivated samples were then used in quantitave-PCR (qPCR) analysis.

2.7 Quantitative PCR (q-PCR)

For qPCR analysis, 4-10 µl of RT reaction product was used. For each reaction, cDNA was combined with 1.85 µg of gene-specific forward and reverse primer, 33 µl of SYBR Advantage qPCR Premix (Clontech) and the reaction volume was brought up to 66 µl with dH_2O. The sample was then mixed by pipetting and aliquoted into 0.2 ml single tubes (ABgene) to make 20 µl triplicates. For each sample, cDNA encoding 5S rRNA was used as an internal control and was prepared as described above in a separate reaction. Rotor-Gene Q was used to carry out the qPCR reaction, which was set up as follows: initial hold at 50°C for 20 seconds and denaturation at 95°C for 10 minutes followed by 40 cycles alternating between denaturation at 95° for 15 seconds and annealing of the primer and extension at 58°C for 60 seconds. The reaction was ended with a final melt at 95°C for 5 minutes. Data were then analyzed with Rotor-Gene Q Series Software and then Ct values were obtained. For each sample, 3 technical replicates and minimum of 3 biological replicates were examined. Comparative quantification algorithm ΔCt was used for quantification of relative Vif RNA levels from the RNA-immunoprecipitation experiment. The calibrator was chosen to be the sample transfected with pc-hVif and the fold difference between Vif RNA in test samples and calibrator was computed as 2^ΔCt.

For quantification of Vif RNA levels in HEK293T cells and H9 lymphocytes transfected with the HIV proviral clone pMenv(-) and pc-hVif, respectively, ΔΔCt method was used. In this

quantification, 5S rRNA was used as the normalizer gene. Both test sample and calibrator samples were adjusted in relation to a normalizer gene Ct from the same two samples. For HEK293T cells, samples transfected with the proviral clone pMenv(-) served as a calibrator sample, whereas for H9 cells, sample transfected with pc-hVif served as a calibrator sample. Mock sample contained RNA harvested from untransfected cells, whereas no RNA sample contained primers only and served as a control for primer amplification.

2.8 Primer extension

2.8.1 Preparation of radiolabelled reverse primers

For primer extension analysis, Vif-specific reverse primers were end-labelled with γ^{33}P-dATP. In a 1.5 ml microtube, 0.2 µg of reverse primer, 50 µCi of γ^{33}P-dATP (Perkin Elmer), 1 µl of 10X T4 polynucleotide kinase buffer (700 mM Tris-HCl pH 7.6, 100 mM $MgCl_2$, 50 mM DTT), 20 units of T4 polynucleotide kinase (New England Biolabs) were combined and the reaction volume was brought up to 10 µl with dH_2O. Sample was incubated for 1 hour at 37°C after which the reaction was stopped by the addition of 1 µl of 0.5M EDTA and diluted with 40 µl of dH_2O. The unincorporated nucleotides were removed by adding the sample to a G-50 centrifuge column (Thermo Scientific) containing 700 µl of G-50 sephadex solution (GE Healthcare) and centrifuging it at 2,700 x g for 2 minutes at room temperature. The flowthrough containing the radiolabelled primer was collected and the sample was stored in -20°C or used in primer extension analysis.

2.8.2 Primer extension

Samples containing cytoplasmic RNA (20-40 μg) harvested from HEK293T cells transfected with pcPAP and pMenv(-) or pc-hVif were combined with 5×10^5 CPM of Vif-specific radiolabelled reverse primer. The reaction volume was brought up to 11 μl with dH_20 and the sample was heated for 5 minutes at 95°C followed by cooling for 2 minutes on ice. The primer was allowed to anneal to the template by incubating the sample for 10 minutes at 58°C followed by incubation for 3-5 minutes at room temperature. Samples was centrifuged to collect all the liquid and 4 μl of 5X first-strand buffer (375 mM KCl, 250 mM Tris-HCl pH 8.3, 15 mM $MgCl_2$, 5 mM DTT), 2 μl 0.1M DTT, 1 μl of 10 mM dNTPs and 40 units of RNase inhibitor (New England Biolabs) were added. Samples were heated for 2 minutes at 48°C after which 20 units of M-MuLV reverse transriptase enzyme (New England Biolabs) were added to the sample and incubated for additional 50 minutes at 48°C. The primer extension reaction was stopped by heating the sample at 70°C for 10 minutes and the addition of 10 μl of RNA loading dye (95% formamide, 20 mM EDTA, 0.25% bromophenol blue, 0.25% xylene cyanol). Prior to loading of the samples on the large sequencing gel (7M urea, 6% acrylamide), the samples were heated for 4 minutes at 90°C and chilled on ice for 2 minutes. From each sample, 6 μl was loaded onto a gel and the RT products were separated at 30 Watts for 2.5-3.5 hours. After electrophoresis, the gel was placed against a thin filter paper and air dried using a gel dryer (Thermo Savant) under a vacuum for 2 hours at 80°C. Next, the dried gel was placed against phosphor imaging screen (BIO-RAD) overnight and scanned in a GE Healthcare Typhoon Trio+ Variable Mode Imager. The resulting image was analyzed with Quantity One 1D-analysis software.

2.9 Sequencing ladder

Manual dideoxynucleotide sequencing was performed to generate ladders that were used to identify the sequence of nucleotides in cDNA products generated in the primer extension analysis. Plasmid template, pMenv(-) or pc-hVif, was denatured by combining 8-16 µg of plasmid DNA with 2 µl of 2M NaOH, 2 µl of 2 mM EDTA and the total volume was brought up to 22 µl with dH_2O. Samples were incubated for 6 minutes at room temperature, after which 2 µl of 2M NH_4OAc pH 4.6 and 75 µl of 95% ethanol were added. Plasmid DNA was precipitated overnight at -20°C followed by centrifugation at 16,000 x g for 20 minutes at 4°C. Next, the supernatant was discarded and the pellet was air-dried and resuspended in 7 µl of dH_2O. Each sample was combined with 2 µl of reaction buffer (250 mM NaCl, 200 mM Tris-HCl pH 7.5, 100 mM $MgCl_2$) and 0.2 µg of the appropriate reverse primer. The primer was annealed by incubating the sample for 2 minutes at 65°C followed by gradual cooling to 35°C over 25-30 minutes period after which the sample was chilled on ice for 5 minutes. Meanwhile, 4 termination tubes were prepared each containing 2.5 µl of one of the dideoxynucleotides. For each sequencing reaction, 1 µl of 0.1 M DTT, 0.4 µl of labeling mix (0.75 µM dGTP, 7.5 µM dCTP, 7.5 µM dTTP), 6.25 µCi of ^{35}S dATP (Perkin Elmer), 3.25 units of Sequenase DNA polymerase (USB Corp.), 1.75 µl of dilution buffer (10 mM Tris-HCl pH 7.5, 5 mM DTT, 0.1 M EDTA), 0.42 µl of dimethyl sulfoxide (DMSO), and 1.6 µl of dH_2O were combined and added to the denatured DNA-containing sample. The reaction was incubated for 5 minutes at room temperature after which 3.5 µl of the sample was aliquoted into each of the 4 termination tubes. Samples were incubated for 5 minutes at 37°C, after which 4 µl of stop solution (95% formamide, 20 mM EDTA, 0.25% bromophenol blue, 0.25% xylene cyanol) was added. Samples were heated at 75°C for 2 minutes and 4 µl of each termination reaction was loaded onto a large sequencing gel alongside primer extension reaction products.

2.10 Protein Isolation

Cell pellets were lysed with 2 volumes of cytoplasmic lysis buffer. Samples were vortexed and placed on ice for 10 minutes, and centrifuged at 14,000 x g for 10 minutes at 4°C to pellet cell debris. Supernatants were transferred to new 1.5 ml microtubes and protein concentrations were determined by Bradford assay (OD_{595} nm). Next, 2X Laemmli buffer (125 mM Tris-HCl pH 6.8, 20% glycerol, 10% β-mercaptoethanol, 4%SDS, 0.25% bromophenol blue) was added and samples were heated at 95˚C for 5 minutes. Denatured protein samples were stored in -20˚C or used in western blot analysis.

2.11 Western blotting

Denatured protein samples were resolved by sodium dodecyl sulphate-polyacrylamide gel electrophoresis (SDS-PAGE). Samples were loaded onto a 12% acrylamide gel and the proteins were separated at 200V for 40 minutes in 1X running buffer (192 mM glycine, 25mM Tris-HCl pH 8.3, 0.1% SDS). Semi-dry transfer (BIO-RAD) was used to transfer the resolved proteins from the gel onto a nitrocellulose membrane (GE Healthcare). The blot was rinsed in western transfer buffer (160 mM glycine, 25 mM Tris-HCl pH 8.3, 20% methanol, 0.02% SDS) prior to the transfer. The gel was placed on top of a nitrocellulose membrane and four pieces of thick chromatography paper (Fisher Scientific) were placed under and over to form a sandwich. Proteins were transferred at 0.12 Amp for each membrane for 40 minutes. Following the transfer, the membrane was blocked with 10 ml of 5% milk in PBS-T (1X PBS with 0.1% Tween 20) for 2 hours by gentle rocking at room temperature. Next, membrane was incubated with the appropriate amount of primary antibody (Table 2) in 5 ml of 5% milk in PBS-T by gentle

Table 2. List of antibodies. Antibodies used in immunoprecipitation and western blotting experiments are listed below.

Antibody	Supplier and catalogue #	Final concentration	Experiment
Rabbit PAP polyclonal	gift of N. Tumer Rutgers University	1:5,000	RNA-immunoprecipitation
Mouse HA monoclonal	Sigma Aldrich H9658	1:20,000	western blot
Mouse HIV-1 Vif monoclonal	NIH #6459	1:2,500	western blot
Mouse HIV-1 Vif monoclonal	Santa Cruz sc-69731	1:500	western blot
Rabbit APOBEC3G polyclonal	NIH #10082	1:10,000	western nlot
Mouse Actin monoclonal	Novus Biologicals NB100-74340	1:5,000	western blot
Rabbit VSV-G polyclonal	GenScript A00199-40	1:5,000	western blot
Anti-Mouse secondary	Sigma Aldrich A9044	1:5,000	western blot
Anti-Rabbit secondary	Sigma Aldrich A4914	1:5,000	western blot

rocking at 4˚C overnight. The membrane was then washed with 1X PBS-T buffer by gentle rocking for 10 minutes. A total of 3 washes was performed after which the membrane was incubated with the appropriate secondary antibody conjugated to a horseradish peroxidase enzyme (Table 2) in 5 ml of 5% milk in 1X PBS-T. The membrane was then washed as described above and incubated with 1.5 ml of enhanced chemiluminescence (ECL) reagent (Perkin Elmer) for 2 minutes at room temperature. The membrane was then exposed to a clear blue x-ray film (Thermo Scientific) for 5-15 minutes and developed in the dark. The membrane was stripped with 10 ml of 8M guanidine hydrochloride (G-HCl) by gentle rocking at room temperature to allow re-probing of the blot with different antibodies. The membrane was washed 3 times with 1X PBS-T with gentle rocking and blocked prior to the addition of different primary antibody. Blocking, incubation with antibodies and washes were performed as described.

2.12 Plasmid transformation

Transformation of plasmid DNA was performed in competent *E.Coli* DH5α cells. Thawed competent cells (100 µl) were mixed with plasmid DNA (0.3-1 µg) by gentle pipetting in 1.5 ml microtube and incubated on ice for 30 minutes. Samples were then heat-shocked for 1 minute at 42˚C and placed on ice for 2 minutes. Next, 300 µL of Luria-Bertani (LB) media was added to each sample and the cells were incubated in the media with shaking at 150 rpm for 1 hour at 37˚C. Following the incubation, the cells were pelleted at 5,000 x g for 10 minutes at room temperature. Supernatant was removed to leave about 100 µl of LB media above the pellet, which was used to resuspend the cells. Resuspended cells were then plated onto LB plates coated with 20 µl of ampicillin (100 µg/µl). Plates were placed into incubator at 37˚C overnight after which colony formation was examined. Colonies were selected and the harvested plasmid DNA

was used for sequencing. Positive colonies were used in large scale plasmid isolation to obtain high yield of purified plasmid DNA.

2.13 Large scale plasmid isolation

LB cultures (4 ml) containing 0.4 µg of ampicillin were inoculated with selected colonies and incubated with shaking at 250 rpm for 18 hours at 37˚C. Next, the overnight 4 ml cultures were transferred to 400 ml LB cultures containing 40 µg of ampicillin and incubated by shaking at 250 rpm at 37˚C for additional 18 hours. The cultures were then transferred to 250 ml Oak Ridge polycarbonate centrifuge bottles and the cells were pelleted by centrifuging the samples at 4,000 x g for 10 minutes at 4˚C. The supernatant was discarded and the pellets were washed by resuspending them in 25 ml of 1X STE (100 mM NaCl, 10 mM Tris-HCl pH 8.0, 1 mM EDTA pH 8.0) followed by centrifugation at 4,000 x g for 10 minutes at 4˚C. The supernatant was discarded and the remaining pellet was resuspended in 10 ml of cold solution 1 (50 mM glucose, 25 mM Tris HCl pH 8.0, 10 mM EDTA). Cells were lysed with the addition of 20 ml of solution 2 (0.2 M NaOH, 1% SDS), vortexed and placed on ice for 4 minutes. Next, 10 ml of solution 3 (3M KOAc, 12% glacial acetic acid) was added and the sample was vortexed and incubated on ice for 10 minutes. Following the incubation, samples were centrifuged at 4,000 x g for 10 minutes at 4˚C and the plasmid DNA-containing supernatants were filtered through 8 layers of cheesecloth. Approximately 20 ml of cold isopropanol was added and the DNA was precipitated at -20˚C for 1 hour. Next, the samples were centrifuged at 4,000 x g for 20 minutes at room temperature and the pellets were air dried for 3 minutes. Pellets were then resuspended in 5 ml of 1X TE buffer (10 mM Tris HCl pH 8.0, 1 mM EDTA) and transferred to 15 ml tubes containing 7 g of cesium chloride (CsCl). Samples were vortexed to dissolve CsCl, additional TE buffer was

added to bring the volume of the solution to 9 ml and 0.5 ml of 10 µg/µl ethidium bromide was added. Samples were mixed throughoutly by vortexing and centrifuged at 4,000 x g for 7 minutes at room temperature. The DNA-containing supernatant was transferred into bell-top ultracentrifuge tube (Beckman) using glass pipette and centrifuged at 155,000 x g for 22 hours at 22˚C. The band containing the supercoiled DNA was extracted with hypodermic needle and the obtained sample was diluted with 1X TE buffer to a final volume of 5 ml. Ethidium bromide was removed from the plasmid DNA-containing sample with 5 washes with isoamyl alcohol. During each wash, 5 ml of isoamyl alcohol was added to the sample, vortexed, the layers were allowed to separate and the top layer was removed. After the last wash, the volume of the sample was brought to 5 ml with 1X TE and 10 ml of 100% ethanol was added. Samples were precipitated overnight at -20˚C and centrifuged at 4,000 x g for 20 minutes at 4˚C. The supernatant was discarded and the remaining pellet was washed twice with 70% ethanol by centrifuging the sample at 4,000 x g for 10 minutes at 4˚C. After discarding the supernatant, the pellet was air-dried and resuspended in 100-500 µl of 1X TE and the DNA was quantified using spectrophotometer at OD 260 nm.

2.14 Virus particle isolation

Viral particles were isolated from media collected from cells transfected with the HIV proviral clone pMenv(-) 44 hours post-transfection. Pseudotyping of viral particles was performed using glycoprotein G of vesicular stomatitis virus by co-transfecting pCMV-VSV-G (1-3 µg) with the pMenv(-) proviral clone. Media containing viral particles was transferred to 1.5 ml microtubes and centrifuged at 9,000 x g for 5 minutes to pellet cell debris. The supernatant was transferred to new 1.5 ml microtube and centrifuged at 16,000 x g for 90 minutes at 4˚C to

pellet viral particles. Supernatant was aspirated and the pellet was resuspended in fresh media. For ELISA analysis, 1X lysis buffer (10% Triton X-100 in Milli-Q H_2O) and sample diluent media (1% BSA, 0.2% Tween 20 in RPMI-1640) were added to the samples.

2.15 Enzyme-linked immunosorbent assay (ELISA)

To quantify viral particles released from HeLa-A3G cells, HIV-1 p24 CA ELISA (National Cancer Institute, Frederick National Laboratory, MA) was used. Viral particles were harvested as described above and 1/10 volume of lysing solution (10% Triton X-100 in Milli-Q H_2O) was added. Samples were vortexed well and incubated for 1 hour at 37°C. Meanwhile, 2-fold serial dilutions of standard ($p24^{CA}$ 40,170 pg/ml) was prepared using sample diluent. ELISA plate was washed 4 times with 1X Wash Concentrate (2 mM imidazole, 160 mM NaCl, 0.02% Tween 20, 0.5 mM EDTA) (KPL) and blotted on a clean paper towel to dry between the washes. After, 100 µl of standards and samples were aliquoted in duplicates into wells. In addition, 2 wells were left empty and 2 wells were filled with sample diluents which served as a blank and a background control, respectively. The plate was then sealed and incubated for 2 hours at 37°C. After incubation, the plate was washed as described above and 100 µl of rabbit anti-HIV-1 (MN) p24 antibody diluted (1:300) in primary antibody diluent (10% FBS, 2% normal mouse serum (NMS) in RPMI-1640) was added to each well except the blank wells. Plate was sealed and incubated for 1 hour at 37°C. After incubation with primary antibody, washes were performed as described above and goat anti-rabbit IgG secondary antibody conjugated to horse radish peroxidase was diluted (1:200) in secondary antibody diluent (5% normal goat serum (NGS), 2% NMS, 0.01% Tween 20 in RPMI-1640) and 100 µl of diluted antibody was added to each well except the blank wells. The plate was sealed and incubated for 1 hour at 37°C. After incubation

with secondary antibody, the plate was washed as described above and 100 µl of 3,3',5,5'-tetramethylbenzidine (TMB) peroxidase substrate (KPL) was added to each well and incubated for 30 minutes at room temperature. The reaction was then stopped with the addition of 100 µl of 1M HCl and the yellow-coloured product was quantified using an ELISA plate reader (Beckman Coulter DTX880 Multimode Detector) at 450 nm absorbance using the Beckman Coulter Multimode Analysis Software. The data were then analyzed with ElisaAnalysis report (ElisaKit) using 4 parameter logistic ELISA curve fitting.

2.16 Infectivity assay

Single-cycle infectivity assays were performed using pseudotyped HIV-1 virions. Pseudotyped virions harvested from PAP, PAPx or pcDNA3 expressing HeLa-A3G cells were quantified by HIV-1 p24 CA ELISA and equal amounts (5 ng) were used to infect 1G5 cells. Infections of 1G5 cells (2.5 x 10^5 cells) were performed in 24-well plate in a presence of 8 µg of polybrene in a final volume of 1.5 ml of DMEM supplemented with 10% FBS. After 20 hours, cells were centrifuged at 200 x g for 7 minutes at 4°C and the supernatant was aspirated. The pelleted cells were washed with 1 ml of 1X PBS by centrifuging at 200 x g for 7 minutes at 4°C. The supernatant was aspirated and the cells were resuspended in 2 ml of fresh media and incubated for additional 24 hours at 37°C. Cells were harvested by centrifugation at 200 x g for 7 minutes at 4°C, the supernatant was aspirated and the cells were lysed with the appropriate lysis buffer.

2.17 Luciferase assay

For the luciferase assay, 50 µl of the 1X Luciferase Cell Culture Lysis Reagent (Promega) was added to pelleted cells and the samples were vortexed for 15 seconds. After, samples were centrifuged at 12,000 x g for 15 seconds at room temperature and the supernatant was transferred to new 1.5 ml microtubes. The lysates were stored in -20°C or used to quantify luciferase expression with a single-tube luminometer with injectors (EG&G Berthold Lumat LB 9507 Ultra Sensitive Tube Luminometer). Cell lysates (20 µl) were aliquoted into 5 ml tubes (Sarstedt) and 100 µl of the Luciferase Assay reagent (Promega) was dispensed into the luminometer tubes. The luminometer was programmed to perform a 2-second measurement delay followed by a 10-second measurement read for luciferase activity.

2.18 PCR for detection of HIV-1 DNA in infected 1G5 cells

Pseudotyped virions harvested from PAP, PAPx or pcDNA3 expressing HeLa-A3G cells were quantified by HIV-1 p24 CA ELISA and equal amounts (10 ng) were used to infect 1G5 cells (2.5×10^5). Cells were washed and resuspended in fresh media 4 hours post-infection. DNA was harvested by adding 100 µl of nuclear lysis buffer (150 mM NaCl, 25 mM Tris-HCl pH 7.6, 1% NP-40, 1% sodium deoxycholate, 0.1% SDS) to cell pellet 24 hours post-infection. PCI extraction was performed, after which DNA was precipitated in 2.5 volumes of 100% ethanol and 1/10 volume of 3M NaOAc. RNA was precipitated at -20°C for 18 hours, followed by centrifugation at 16,000 x g for 30 minutes at 4°C. The supernatant was discarded and the pellet was washed with 70% ethanol by centrifuging the samples at 16,000 x g for 15 min at 4°C. HIV-

1 DNA was amplified using Vif-specific primers (Table 1). DNA fragment encoding 5S rRNA was amplified using 5S rRNA-specific primers (Table 1), which served as a loading control.

3. RESULTS

3.1 PAP depurinates rRNA without causing cell toxicity

PAP is known to depurinate a specific adenine residue (A4324) within the conserved α-sarcin/ricin loop in the eukaryotic 28S rRNA. To confirm the expression and activity of PAP in HeLa-A3G cells, pc-PAP construct encoding 3X-FLAG-tagged PAP was transiently transfected and primer extension was carried out to determine if 28S rRNA was depurinated. A construct encoding a catalytically inactive mutant of PAP, pcPAPx, was used as a control. PAPx has a point mutation in the active site (E176V) which abolishes its ability to depurinate RNA (Hur et al. 1995). Expression of wild-type PAP resulted in depurination of 28S rRNA as shown by a band indicating termination of primer extension at the predicted adenine residue (Figure 7A). By comparing the intensity of the band at A4324 relative to total 28S rRNA, it was estimated that PAP depurinated approximately 15% of the rRNA. As expected, PAPx did not depurinate 28S rRNA (Figure 7A).

In addition, to confirm that the expression of PAP at the concentration used in the experiments (0.5 - 1 μg) was not toxic to HeLa-A3G cells, an MTT conversion assay was performed. Cells transfected with pcPAP showed no decline in cell viability compared to cells transfected with pcPAPx or pcDNA3, an empty vector (Figure 7B). Therefore, PAP was efficiently expressed in HeLa-A3G cells and did not cause cytotoxicity at the concentration used.

3.2 PAP associates with Vif RNA *in vivo*

To determine whether PAP associates with Vif RNA *in vivo,* immunoprecipitation of PAP-bound RNA followed by RT-qPCR with Vif-specific primers was performed. HEK293T cells were transfected with pcPAP and pc-hVif, encoding codon-optimized Vif for efficient

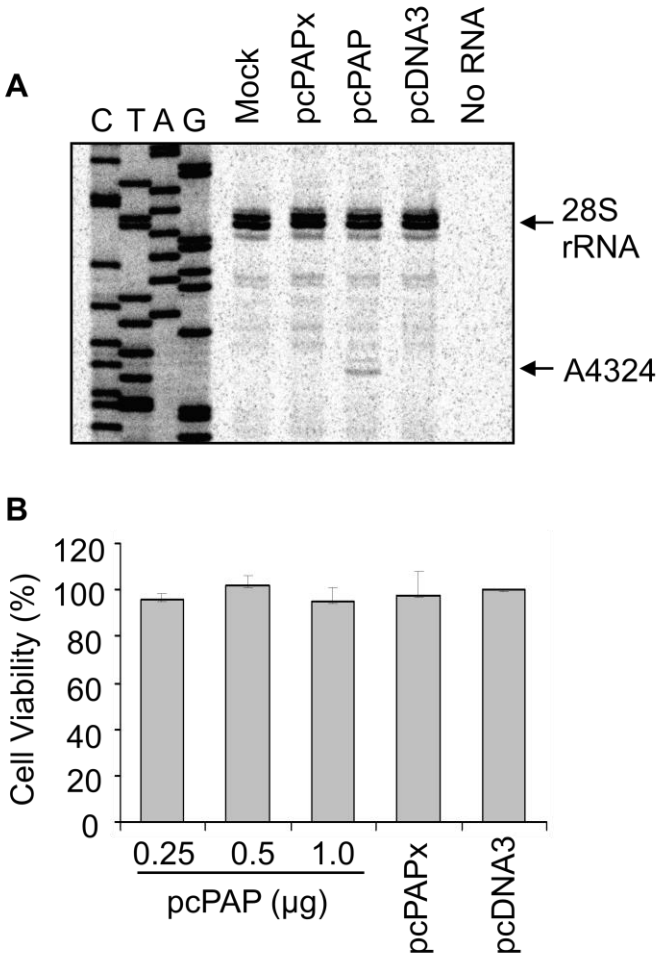

Figure 7. PAP depurinates rRNA without cell toxicity. (A) HeLa-A3G cells were transfected with pMenv(-) (5 μg) and pcPAP or pcPAPx (1 μg). Cells were harvested 44 hours post-transfection and primer extension was performed on cytosolic RNA (3 μg) to determine the level of rRNA depurination relative to the total amount of 28S rRNA. Dideoxynucleotide sequencing of 28S rDNA with the same primer (28S rRNA dep R) used for primer extension confirmed the location of rRNA depurination by PAP. Another primer (28S rRNA R) was used as a control for total 28S rRNA in each sample. Mock represents untransfected cells. **(B)** Viability of cells expressing PAP or PAPx was tested by an MTT conversion assay 48 hours post-transfection. Values are presented as ratios relative to samples transfected with pcDNA3 for 3 independent experiments.

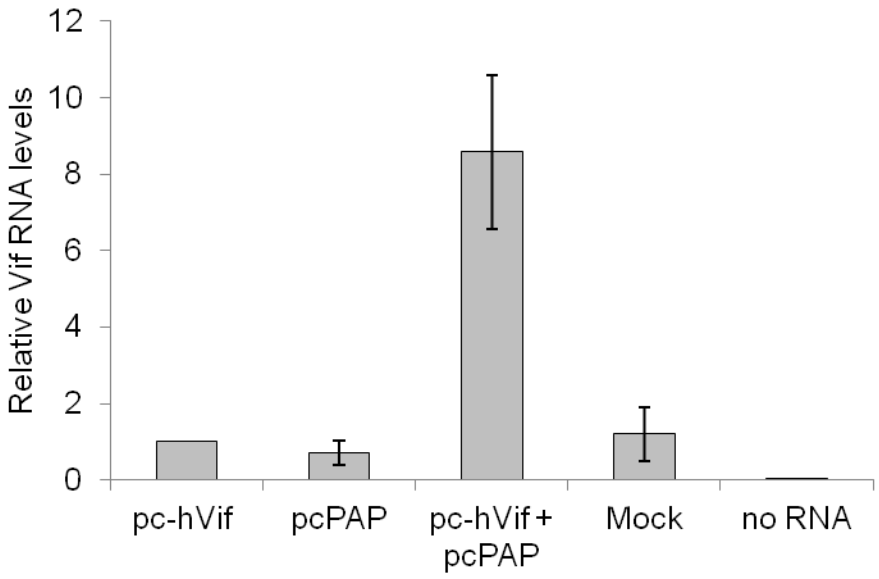

Figure 8. PAP associates with Vif RNA *in vivo.* HEK293T cells were transfected with pc-hVif (3 μg) and pcPAP (2.5 μg). Cells were crosslinked by UV and lysed 44 hours post transfection. Immunoprecipitation was performed on cell lysates incubated with magnetic beads coated with PAP polyclonal antibody. RNA was extracted from beads and used in RT-qPCR with Vif-specific primers (hVif 431F and hVif 579R). Mock sample contained untransfected cells, while no RNA sample contained primers only. Values are the means ± S.E. of 3 independent experiments.

expression. This cell line was chosen due to its high transfection efficiency and the codon-optimized vector, pc-hVif, was used to achieve high expression of Vif RNA. Immunoprecipitation was performed with magnetic beads coated with PAP polyclonal antibody. RNA was harvested from the beads and RT-qPCR analysis was performed using Vif-specific primers (Table 1). Samples co-transfected with pcPAP and pc-hVif showed approximately 8-fold higher Vif RNA levels compared to samples transfected with pcPAP or pc-hVif alone (Figure 8). Mock sample contained untransfected cells, and no RNA sample served as a control for primer amplification. Overall, *in vivo* RNA pulldown assay showed association of PAP with Vif mRNA.

3.3 PAP decreases Vif mRNA and protein levels.

3.3.1 PAP decreases Vif mRNA levels, which is partially rescued by the overexpression of Rev.

In order to determine the effect of PAP on Vif mRNA expressed from the HIV-1 proviral clone pMenv(-), RT-qPCR was performed on cytosolic RNA using Vif-specific primers (Table 1). The plasmid encoding pMenv(-) is derived from the HXB2 HIV-1 strain, but is unable to express *env* gene due to mutation in its start codon (Sadaie et al. 1992). HEK293T cells were transfected with pcPAP, pcRev encoding the regulatory HIV-1 protein Rev, and pMenv(-). RT-qPCR using Vif-specific primers allowed me to determine if the expression of PAP alters the levels of the 4 kb mRNA from which Vif is expressed, as well as the full-length 9 kb RNA, since Vif ORF is present in both transcripts. Depurination in a region of Vif ORF that is being reverse transcribed would cause stalling of the enzyme. Therefore, only non-depurinated mRNA containing Vif ORF would be reverse transcribed and amplified through RT-qPCR. PAP

Figure 9. PAP decreases the levels of Vif mRNA and protein. (A) HEK293T cells were transfected with pMenv(-) (5 μg), pcPAP (2.5 μg) and pcRev (2.5 μg). Cells were harvested 44 hours post transfection and cytosolic RNA (1-3 μg) was extracted for RT-qPCR analysis with Vif-specific primers (HXB2 5200F and HXB2 5350R). The levels of Vif mRNA were standarized relative to 5S rRNA. Mock sample represents untransfected cells, and no RNA serves as a negative control for primer amplification. **(B)** HEK293T cells were transfected with pMenv(-) (5 μg), pcPAP (2.5 μg) and pcRev (2.5 μg). Cytoplasmic proteins were harvested 40 hours post transfection and analyzed by western blotting. Protein samples (200 μg) were separated on a 12% SDS-PAGE, transferred to nitrocellulose and probed with Vif-specific monoclonal antibody (1:500) and β-actin-specific monoclonal antibody (1:10,000), which was used as a loading control. Mock sample served as a negative control since it contained untransfected cells. Blot is a representative of 3 independent experiments. **(C)** H9 lymphocytes were transfected with pc-hVif (3 μg) and pcPAP (1 μg). Cells were harvested 44 hours post-tranfection and cytosolic RNA (1-3 μg) was extracted for RT-qPCR analysis using Vif-specific primers (hVif 173F and hVif 383R). The levels of Vif mRNA were standarized relative to 5S rRNA. Values are the means ± S.E. of 3 independent experiments.

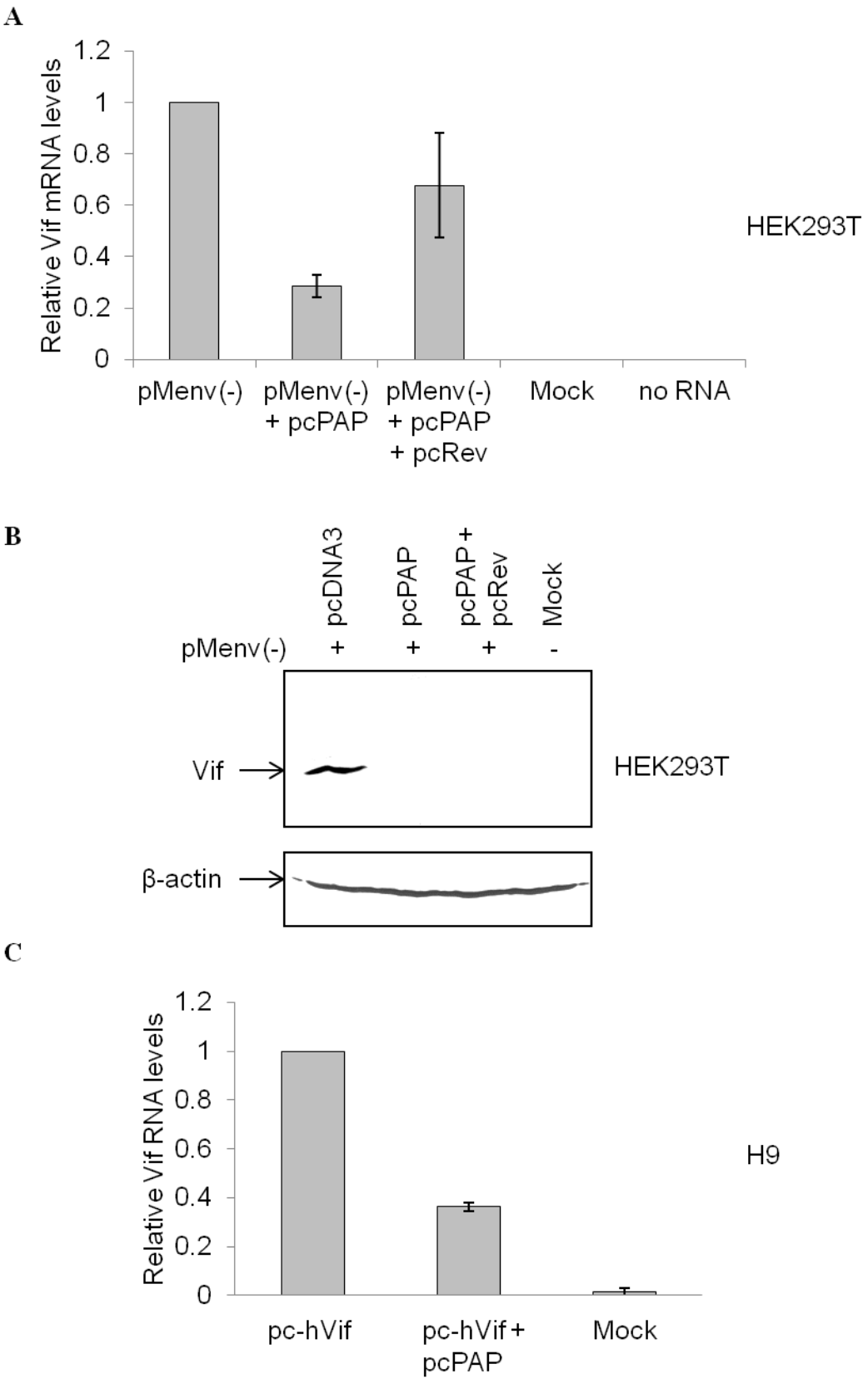
A
Relative Vif mRNA levels
1.2
1
0.8
0.6
0.4
0.2
0
pMenv(-)
pMenv(-) + pcPAP
pMenv(-) + pcPAP + pcRev
Mock
no RNA
HEK293T
B
pcDNA3
pcPAP
pcPAP + pcRev
Mock
pMenv(-)
+
+
+
-
Vif
HEK293T
β-actin
C
Relative Vif RNA levels
1.2
1
0.8
0.6
0.4
0.2
0
pc-hVif
pc-hVif + pcPAP
Mock
H9

decreased the levels of cytosolic Vif mRNA 3-fold compared to cells transfected with pMenv(-) (Figure 9A). Therefore, in the presence of PAP, levels of cytoplasmic intact Vif mRNA were reduced. The export of 4-kb and 9-kb mRNAs from the nucleus is dependent on Rev, which is encoded by the 2-kb class of mRNAs. Reduced levels of Vif mRNA in the presence of PAP could be due to PAP targeting the 2-kb transcripts from which Rev is expressed and subsequent inhibition of nuclear export of the 4-kb transcripts. Therefore, the effect of Rev overexpression when pcPAP and pMenv(-) were co-transfected was tested. Overexpression of pcRev in the presence of PAP resulted in 2-fold increase in Vif mRNA levels, but did not fully recover Vif mRNA levels (Figure 9A).

3.3.2 PAP inhibits Vif protein expression, which is not rescued by the overexpression of Rev.

In order to analyze Vif protein levels in samples transfected with pMenv(-), pcPAP, and pcRev, western blotting was performed using cytosolic proteins harvested 40 hours post transfection. A sample transfected with pMenv(-) alone showed a band that agreed with the molecular weight of Vif (Figure 9B). This band was not detected in samples co-transfected with pcPAP and pcRev, (Figure 9B), suggesting that overexpression of Rev in the presence of PAP did not rescue Vif protein expression.

3.33 PAP reduces Vif RNA levels in H9 lymphocytes

In addition, I wanted to determine the effect of PAP on Vif mRNA levels in a lymphocytic cell line, which would be more biologically relevant since HIV-1 naturally infects CD4+ T cells and macrophages. The lymphocytic cell line used was H9, which expresses A3G endogenously. Relative Vif mRNA levels expressed from the pc-hVif clone were determined by RT-qPCR using hVif-specific primers (Table 1). The codon-optimized clone was used in H9

cells instead of the proviral clone to achieve high Vif RNA expression despite low transfection efficiency of the lymphocytic cell line. PAP expression caused approximately 3-fold reduction in Vif mRNA levels (Figure 9C). Therefore, the results obtained in H9 lymphocytes supported the trends observed with HEK293T cells, indicating that PAP reduces intact Vif mRNA levels, present either as an ectopically expressed RNA or from the context of the HIV-1 genome.

3.4 PAP depurinates Vif ORF when expressed from pc-hVif or pMenv(-).

Since PAP is an N-glycosidase and reduction in intact Vif mRNA levels was observed in the presence of PAP, I wanted to determine whether PAP depurinates Vif mRNA. Primer extension was performed to investigate whether the downregulation of Vif mRNA levels could be due to depurination of Vif ORF. HEK293T cells were transfected with pcPAP and pc-hVif or pMenv(-). Transfection of pc-hVif tested whether PAP targeted Vif mRNA in the absence of other HIV-1 proteins, whereas transfection of pMenv(-) allowed determination of potential depurination sites within Vif ORF in the context of the native 4-kb mRNA. Samples were co-transfected with pcPAP or pcDNA3, an empty vector used as a control. Total RNA was extracted 40 hours post transfection and used in primer extension with a radiolabelled reverse primer that annealed to Vif ORF (362-383 for hVif and 5435-5460 for HXB2 Vif). The cDNA products were separated by electrophoresis and visualized by autoradiography. The presence of cDNA of shorter length compared to full length extension in samples co-transfected with pcPAP would suggest a possible depurination site as reverse transcriptase pauses at apurinic sites, leading to termination of primer extension. After performing primer extension of RNA isolated from samples co-transfected with pc-hVif and pcPAP, I detected a band corresponding to a unique

Figure 10. PAP depurinates Vif RNA. HEK293T cells were transfected with pcPAP (2.5 μg) and either **(A)** pc-hVif (3μg) or **(B)** pMenv(-) (5 μg). Cytoplasmic RNA was extracted 44 hours post transfection for primer extension analysis (20 or 40 μg) with radiolabelled primer complementary to a region of Vif ORF (362-383 for hVif and 5435-5460 for HXB2 Vif). cDNA products were separated on 7M urea, 6% acrylamide gel and visualized by autoradiography. Sequencing ladders were generated by manual dideoxynucleotide sequencing of either pc-hVif or pMenv(-) using the same reverse primers. Gels are represenative of 5 independent experiments. **(C)** Schematic diagram of the locations of depurination found in Vif RNA expressed from either pc-hVif or the proviral clone pMenv(-). The numbering is based on the HIV-1 HXB2 strain (accession number K03314.5).

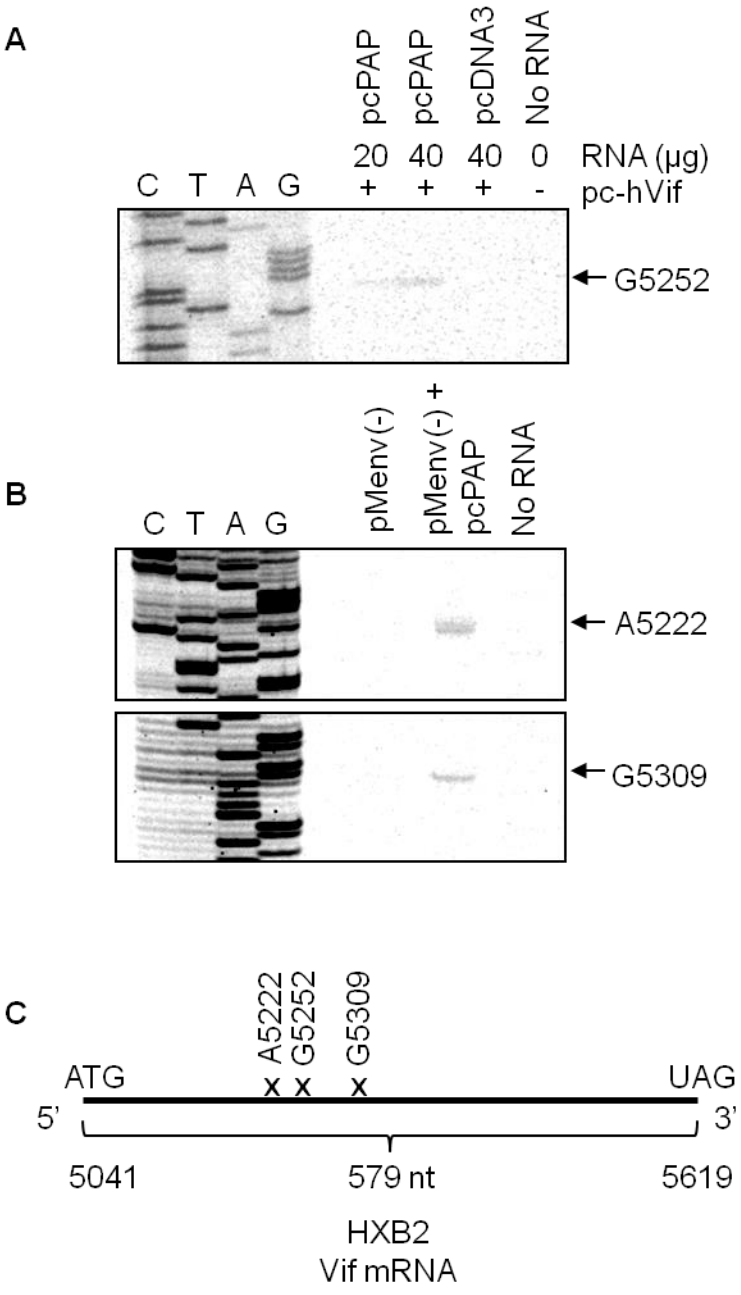
A
pcPAP
pcPAP
pcDNA3
No RNA
20
40
40
0
RNA (µg)
C T A G
+
+
+
-
pc-hVif
G5252
B
pMenv(-)
pMenv(-) + pcPAP
No RNA
C T A G
A5222
G5309
C
A5222
G5252
G5309
ATG
UAG
5'
3'
5041
579 nt
5619
HXB2
Vif mRNA

termination of primer extension. Comparison of this band to a sequencing ladder generated by manual dideoxynucleotide sequencing of pc-hVif showed that reverse transcriptase stalled immediately 3' to (before) a guanine (G) residue (G5252 relative to HXB2 genome or G212 relative to hVif) found within Vif ORF (Figure 10A). This depurination band was observed consistently in several independent experiments.

Primer extension performed on samples co-transfected with pMenv(-) and pcPAP revealed depurination sites at specific adenine (A5222) and guanine (G5309) residues found in Vif ORF present in the HIV-1 HXB2 strain genome (Figure 10B). The 2 depurination bands were observed consistently in several independent experiments and differed from the depurination site detected in hVif mRNA. Overall, primer extension analyses revealed that Vif RNA is a template for depurination by PAP when expressed from either pc-hVif or pMenv(-) constructs.

3.5 Both HIV-1 Vif and hVif downregulate levels of A3G.

Vif is known to inhibit the activity of the cellular cytidine deaminase A3G by targeting it for destruction (Yu et al. 2003, Sheehy et al. 2003, Stopak et al. 200). In order to confirm that Vif expressed from both pMenv(-) and pc-hVif is able to decrease the levels of A3G in HEK293T cells, cells were co-transfected with pMenv(-) or pc-hVif and HA-tagged A3G. Samples transfected with pMenv(-) or pc-hVif showed a single band of approximately 23 kDa, which agreed with the molecular weight of Vif protein (Figure 11). Transfection of HA-A3G alone resulted in a band of approximately 46 kDa, corresponding with the known molecular weight of A3G enzyme (Figure 11). Co-transfection of either pMenv(-) or pc-hVif with HA-

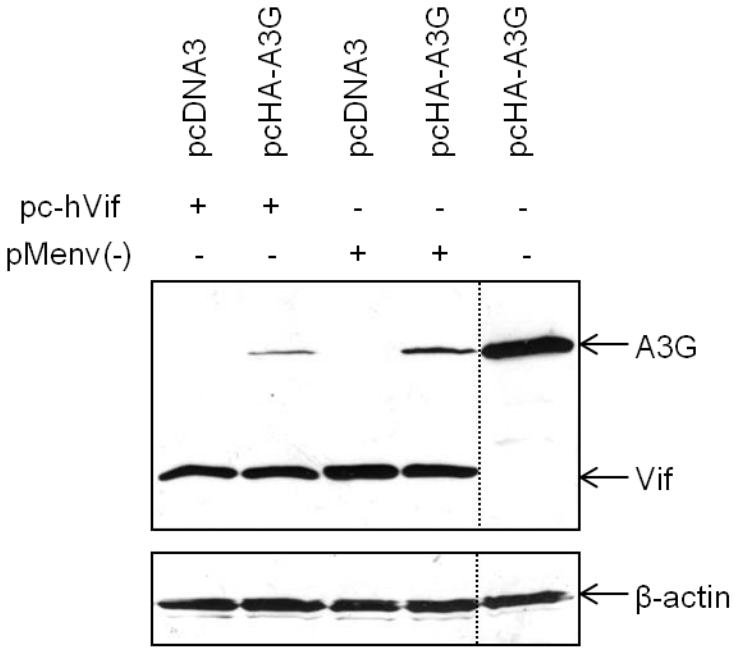

Figure 11. Vif decreases A3G levels in HEK293T cells. Cells were co-transfected with pMenv(-) (5 µg) or pc-hVif (2.5 µg) and pcHA-A3G (2.5 µg) and total cytosolic proteins were harvested 44 hours post-transfection. Protein samples (100 µg) were separared on a 12% SDS-PAGE and analyzed by western blotting using Vif-specific (1:2,500), HA-specific (1:20,000) and β-actin-specific (1:5,000) monoclonal antibodies. B-actin served as a loading control. The dashed line indicates removal of lanes from the gel. Blot is representative of 3 independent experiments.

tagged A3G A3G showed a band corresponding to Vif protein of the same intensity, but much thinner band for HA-A3G, suggesting that Vif is able to downregulate A3G in these cells (Figure 11). Therefore, expression of Vif from pMenv(-) or pc-hVif generated a functional Vif protein.

3.6 PAP, but not PAPx, decreases Vif protein levels when expressed from pc-hVif or pMenv(-) constructs.

Next, I wanted to further investigate the effect of PAP on Vif protein expression. pMenv(-) or pc-hVif were transfected into HEK293T cells along with pcPAP or pcPAPx. Comparing levels of Vif expressed from pMenv(-) and pc-hVif in the presence of pcPAP allowed me to determine whether downregulation of Vif by PAP was dependent on other proteins encoded by HIV-1 or whether PAP could decrease Vif protein levels when transfected alone. Protein samples isolated from cells transfected with pMenv(-) or pc-hVif showed a single band of approximately 23 kDa, corresponding to Vif protein (Figure 12). Co-transfection of pMenv(-) or pc-hVif with pcPAP resulted in a decrease of Vif protein to undetectable levels. In contrast, co-transfection of pcPAPx, a mutant lacking catalytic activity, did not change the levels of Vif protein in either the pMenv(-) or pc-hVif sample (Figure 12). The mock sample served as a negative control, since it contained untransfected cells.

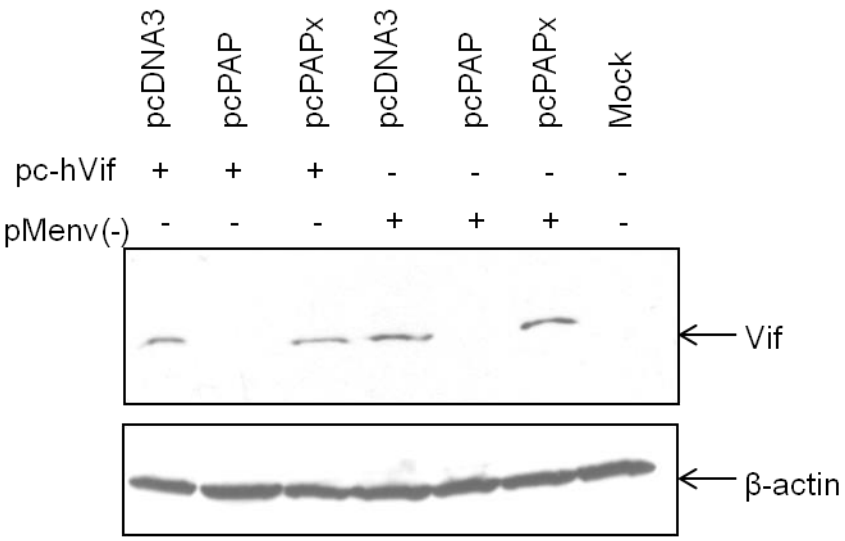

Figure 12. PAP decreases levels of Vif protein when expressed from pc-hVif or pMenv(-). HEK293T cells were co-transfected with pc-hVif (2.5 µg) or pMenv(-) (5 µg) and pcPAP or pcPAPx (2.5 µg). Mock sample contained untransfected cells. Cytosolic proteins were harvested 40 hours post-transfection and used for western blotting analysis (100 µg). Samples were separated on 12% SDS-PAGE gel, transferred to nitrocellulose, and the blot was probed with Vif-specific monoclonal antibody (1:2,500) and β-actin-specific monoclonal antibody (1:10,000), which was used as a loading control. Blot is representative of 3 independent experiments.

3.7 Decreased levels of Vif in the presence of PAP result in elevated levels of A3G in HeLa-A3G cells.

Knowing that PAP downregulates Vif, I wanted to see if this leads to elevated A3G levels since Vif induces degradation of A3G. To explore the effect of PAP on A3G, I used HEK293 and HeLa cells stably expressing A3G. These cells lines were chosen since the A3G gene is stably integrated and therefore variation in the expression levels is minimized compared to differences introduced during transient expression. Transfection of pc-hVif resulted in decreased A3G levels in both cells lines, which agrees with Vif's role in degradation of A3G (Figure 13A and C). Co-transfection of pcPAP resulted in decreased Vif levels and the amount of A3G returned to original levels in both cell lines (Figure 13A and C). Therefore, PAP downregulation of Vif leads to increased levels of A3G, an enzyme involved in host anti-viral response against HIV-1. Transfection of pcPAP or pcPAPx alone did not alter levels of A3G (Figure 13A and C). A3G levels were also decreased in both cell lines when pMenv(-) was transfected and rescued by the addition of pcPAP (Figure 13B and D).

3.8 PAP decreases HIV-1 viral particle release.

To examine the effect of PAP on viral particle release, HeLa-A3G cells were transfected with pMenv(-) and a gradient of pcPAP (0.25-1 μg). HeLa-A3G cells were used instead of HEK293-A3G cells due to their better transfection efficiency. Viral particles were collected from the media 44 hours post transfection and used in p24 ELISA analysis to quantify the amounts of HIV-1 virions released from PAP, PAPx or pcDNA3-expressing cells. PAP decreased HIV-1 viral particle release by approximately 100-fold at the highest PAP concentration tested compared to PAPx or pcDNA3 controls (Figure 14). Inhibition of HIV-1 particle release by PAP

Figure 13. Decreased levels of Vif in the presence of PAP correlate with increased levels of A3G. (A) HEK293 cells stably expressing HA-A3G were transfected with pc-hVif (3 µg) and pcPAP or pcPAPx (1 µg). Cytosolic proteins were harvested 44 hours post transfection and used for western blot analysis (100 µg). Protein samples were separated on 12% SDS-PAGE, transferred to nitrocellulose, and the blot was probed with Vif-specific (1:500), HA-specific (1:20,000) and β-actin-specific (1:10,000) monoclonal antibodies. B-actin was used as a loading control. **(B)** HEK293 cells stably expressing HA-A3G were transfected with pMenv(-) (5µg) and pcPAP or pcPAPx (1 µg). **(C)** HeLa-A3G cells were transfected with pc-hVif (3 µg) and pcPAP or pcPAPx (1 µg). **(D)** HeLa-A3G cells were transfected with pMenv(-) (5µg) and pcPAP or pcPAPx (1 µg). Blot was probed A3G-specific antibody (1:10,000) and the same Vif and β-actin-specific antibodies as listed above. Each blot is representative of 5 independent experiments.

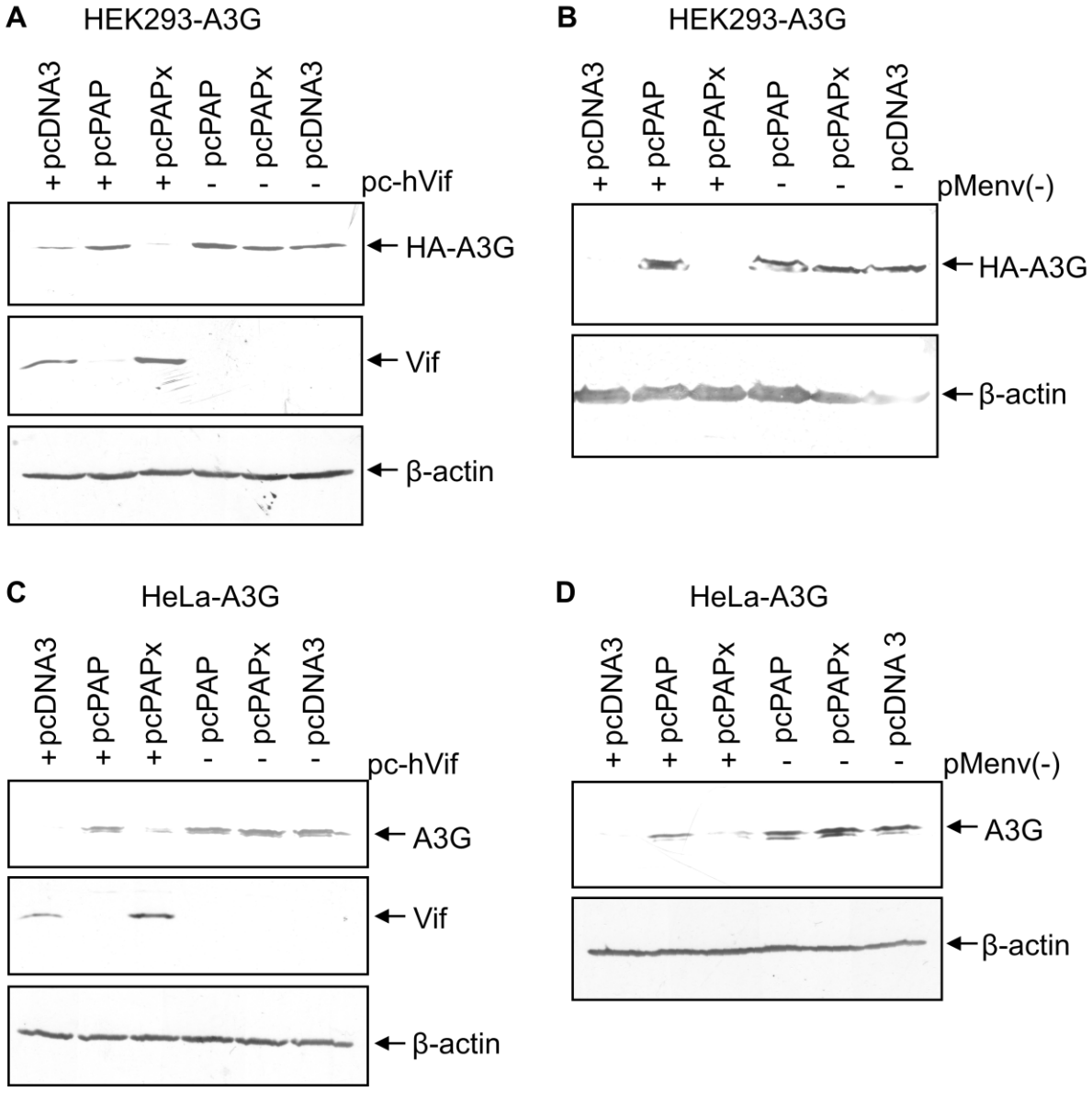
A
HEK293-A3G
+ pcDNA3
+ pcPAP
+ pcPAPx
- pcPAP
- pcPAPx
- pcDNA3
pc-hVif
HA-A3G
Vif
β-actin
B
HEK293-A3G
+ pcDNA3
+ pcPAP
+ pcPAPx
- pcPAP
- pcPAPx
- pcDNA3
pMenv(-)
HA-A3G
β-actin
C
HeLa-A3G
+ pcDNA3
+ pcPAP
+ pcPAPx
- pcPAP
- pcPAPx
- pcDNA3
pc-hVif
A3G
Vif
β-actin
D
HeLa-A3G
+ pcDNA3
+ pcPAP
+ pcPAPx
- pcPAP
- pcPAPx
- pcDNA 3
pMenv(-)
A3G
β-actin

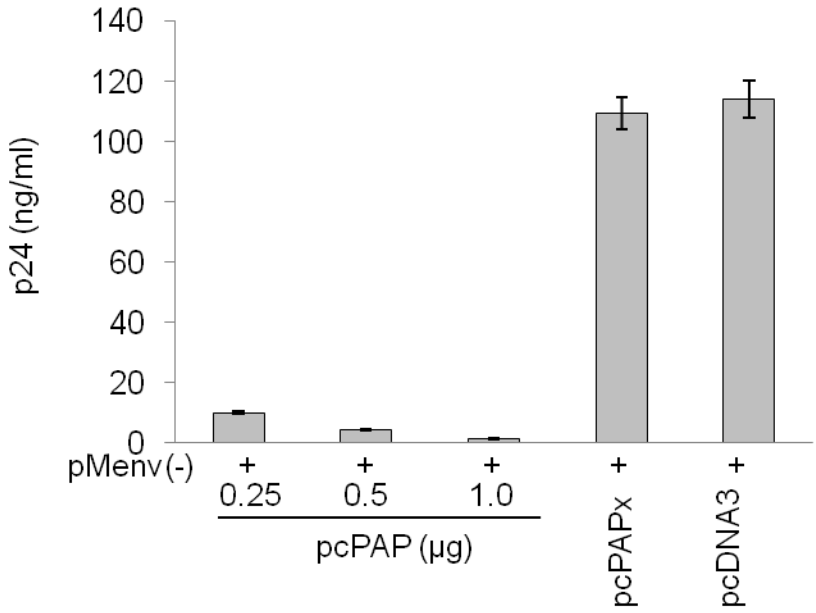

Figure 14. PAP decreases HIV-1particle release from HeLa-A3G cells. HeLa-A3G cells were transfected with pMenv(-) (3 µg) and pcPAP (0.25-1.0 µg), pcPAPx (1.0 µg) or pcDNA3 (1.0 µg). Viral particles were collected from the media 44 hours post transfection and HIV-1 Gag p24 levels were quantified by ELISA. Values are means ± S.E. of 3 independent experiments.

occurred in a concentration-dependent manner (Figure 14). Performing ELISA on HIV-1 particles released from PAP, PAPx or pcDNA3 expressing cells also allowed quantifying and equalizing the amount of virus used in subsequent experiments.

3.9 PAP reduces infectivity of released HIV-1 virions and decreases HIV-1 proviral DNA levels in target cells.

Since PAP downregulates Vif resulting in rescue of A3G levels, I wanted to examine the effect of elevated levels of A3G in the presence of PAP on virus infectivity. Viral particles were pseudotyped using glycoprotein G of vesicular stomatitis virus (VSV-G) and used to infect 1G5 cells. HIV-1 LTR activation was assessed by measuring luciferase activity in cell lysates. Activation of LTR requires efficient expression of HIV-1 regulatory protein Tat and therefore successful infection and expression of HIV-1 RNAs and proteins are required for luciferase expression. VSV-G pseudotyped virions were produced in HeLa-A3G cells by co-transfection of pMenv(-), p-CMV-VSV-G and pcPAP, pcPAPx or pcDNA3. Virions from PAP-expressing cells were approximately 11-fold less infectious, as indicated by decreased luciferase activity, compared to virions from pcPAPx or pcDNA3-expressing cells. Therefore, PAP reduces HIV-1 particle release and the released viral particles are less infectious.

Packaging of A3G into HIV particles in the absence of Vif is associated with decreased HIV-1 reverse transcript accumulation and DNA hypermutation (Harris et al. 2003, Mangeat et al. 2003, Yu et al. 2004, Zhang et al. 2003). Since HIV-1 particles released in the presence of PAP are less infectious, I wanted to examine the effect of PAP in producer HeLa-A3G cells on the levels of integrated HIV-1 DNA in target cells. Pseudotyped HIV-1 virions released from

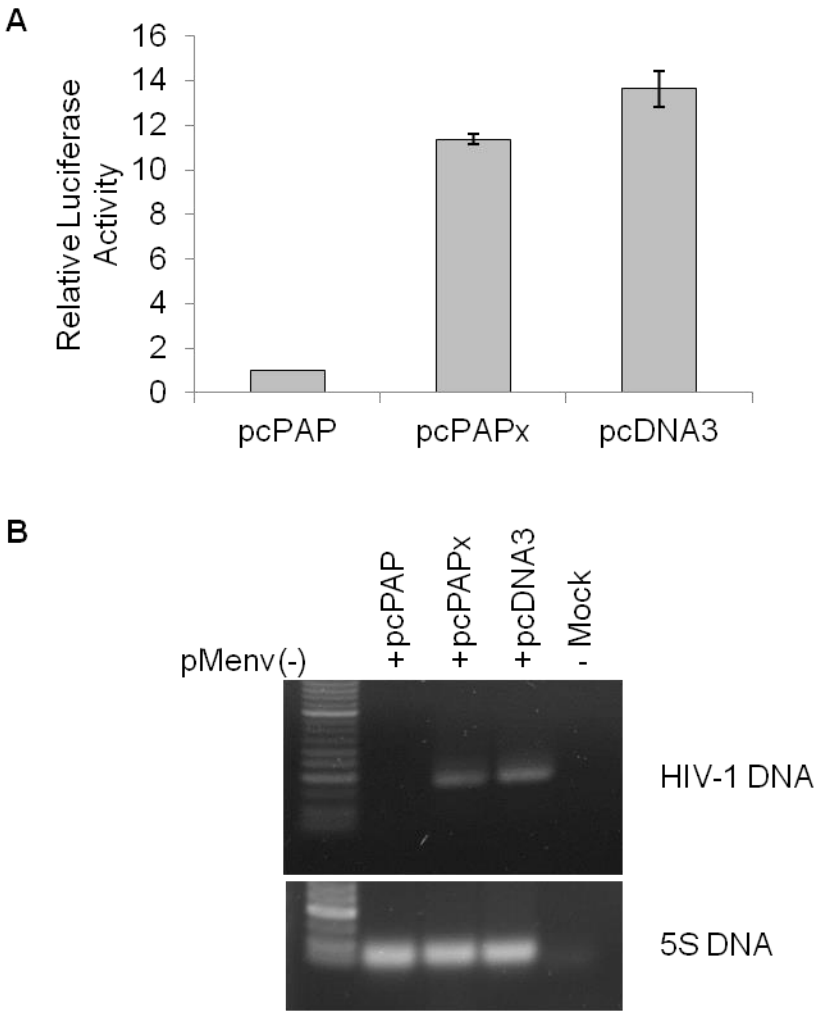

Figure 15. PAP decreases infectivity of HIV-1 virions and lowers the amount of integrated HIV-1 DNA in target cells. (A) HeLa-A3G cells were co-transfected with pMenv(-) (3 µg), p-CMV-VSV-G (1.0 µg) and pcPAP, pcPAPx or pcDNA3 (0.5 µg). Viral particles were collected from the media 44 hours post-transfection and HIV-1 Gag p24 levels were quantified by ELISA. Equal amounts of pseudotyped virus (5 ng) were used to infect 1G5 cells (1.0 x 10^5 cells). Following 40 hours of incubation, cells were collected, lysed and luciferase activity was measured to to determine relative virus infectivity. Renilla lucirefase units (RLU) obtained from cells co-transfected with pcPAP, pcPAPx or pcDNA3 were subtracted from RLU values from mock sample which contained untransfected cells. The relative luciferase activity was obtained as a ratio of RLU values from pcPAPx or pcDNA3 expressing cells to pcPAP expressing cells. Values are means ± S.E. of 3 independent experiments. **(B)** 1G5 cells were infected with viral particles released from pcPAP, pcPAPx or pcDNA3 expressing cells as described above and the presence of integrated HIV-1 DNA was determined by PCR analysis 24 hours post-infection using Vif specific primers (HXB2 5200F and HXB2 5350R).

HeLa-A3G cells transfected with pcPAP, pcPAPx or pcDNA3 were quantified by ELISA and 10 μg was used to infect 1G5 cells. DNA was harvested from cells 24 hours post infection and used in PCR analysis with Vif-specific primers. A band corresponding to the expected product size of approximately 150 nucleotides was seen in samples infected with virions produced from pcPAPx and pcDNA3-expressing cells (Figure 15B). There was no product visible in cells infected with virions released from PAP-expressing cells (Figure 15B). Therefore, the expression of PAP in producer HeLa-A3G cells lowered the amount of integrated HIV-1DNA in infected Jurkat cells.

4. DISCUSSION

4.1 PAP as an antiviral agent

Previous studies have shown that pokeweed antiviral protein (PAP) has a broad anti-viral activity against different plant and animal viruses. Because of its ability to inhibit replication of some animal viruses, including human immunodeficiency virus type 1 (HIV-1), human T cell leukemia virus 1 (HTLV-1) and herpes simplex virus (HSV), PAP has been of a great interest to many researchers and its application as a biotherapeutic agent has been pursued (Zarling et al. 1990, Rajamohan et al. 1999, Mansouri et al. 2009, Teltow et al. 1983, Aaron and Irvin 1980). Initially, the inhibition of virus replication was attributed to rRNA depurination, resulting in the reduction of host cell translation (Foà-Tomasi et al. 1982). Ribosome depurination induces ribotoxic stress response, which can result in apoptosis (Narayanan et al. 2005). However, it was shown previously that ribosome depurination following expression of a RIP in yeast was not sufficient to induce cell death (Li et al. 2007). The ability of PAP to target and depurinate HIV-1 RNAs and inhibit virus production without causing cytotoxicity (Zarling 1990, Rajamohan et al. 1999) suggested an alternative mechanism of virus restriction. In addition, a C-terminal mutant of PAP retained its anti-viral activity, but was unable to depurinate ribosomes, indicating that rRNA depurination might be separable from PAP effect on viruses (Tumer et al. 1997).

Exploiting the anti-HIV activity of PAP, immunoconjugates consisting of the antiviral protein and antibodies targeted to antigens present on helper T cells were tested for their ability to inhibit HIV-1 replication and decrease viral burden (Zarling et al. 1990, Erice et al. 1993, Uckun et al. 1999). PAP-antibody conjugates were found to severely restrict HIV-1 production at picomolar concentrations while causing minimal toxicity (Zarling et al. 1990). Administration of PAP-containing immunoconjugates to chimpanzees and HIV-1 infected human patients showed

promising results, including decreased HIV-1 RNA levels; however, no sustained therapeutic effect was achieved (Uckun et al.1999).

The studies conducted in our lab showed that PAP inhibits HIV-1 protein expression and decreases viral particle release in HEK293T cells by approximately 450-fold (Mansouri et al. 2012). However, HIV-1 particles released from PAP-expressing cells were 7-fold more infectious (Mansouri et al. 2012). The host deaminase enzyme APOBEC3G (A3G) endogenously expressed in CD4+ T cells and macrophages severely restricts replication of HIV-1 mutants lacking functional viral infectivity factor (*vif)* gene and decreases infectivity of the virions (Strebel et al. 1987, Harris et al. 2003, Mangeat et al. 2003, Zhang et al. 2003, Lecossier et al. 2003). A3G is not expressed in adherent cell lines such as HEK293T cells and therefore the impact of PAP on immune defense provided by A3G was not considered in the study performed by Mansouri et al. 2012. In addition, since PAP was shown to depurinate different HIV-1 RNAs (Zhabokritsky et al. 2014), the goal of my study was to determine if PAP depurinates Vif mRNA and its subsequent impact on the cellular innate immunity mediated by A3G. To do this, I investigated the effect of transient expression of PAP on Vif and A3G protein levels in cell lines stably expressing A3G, in addition to assessing virion production and infectivity.

4.2 Depurination of rRNA by PAP is not toxic to cells.

The well documented substrate of PAP is the rRNA, and *in vitro* studies have shown that depurination of rRNA inhibits the binding of elongation factor-2 (EF-2) to ribosomes, causing toxicity to cells through general inhibition of cellular translation (Gessner and Irvin 1980, Nilsson and Nygard 1986). Toxicity has been posited as the mechanism of antiviral activity, as

cell death would limit virus production (Foà-Tomasi et al. 1982). Expression of PAP in HeLa-A3G cells resulted in depurination of 28S rRNA at the predicted adenine (A4324) (Figure 7A). Moreover, the level of rRNA depurination was approximately 15%, which agrees with previous studies (Chan Tung et al. 2008, Mansouri et al. 2012). Studies conducted in HEK293T cells showed similar level of ribosome depurination and demonstrated that this degree of depurination is not sufficient to inhibit the rate of cellular translation (Mansouri et al. 2009, Chan Tung et al. 2008). In addition, PAP did not affect the viability of HeLa-A3G cells as shown by the MTT assay performed on the cells transfected with a gradient of PAP (Figure 7B). Therefore, these findings suggested that depurination of viral RNAs, rather than cellular translation machinery is responsible for the antiviral effect of PAP and the degree of ribosome depurination associated with the transient expression of PAP was not sufficient to induce cell death.

4.3 PAP binds and decreases the levels of Vif mRNA and protein

Zhabokritsky et al. previously showed that PAP depurinates regulator of expression of virion proteins (*rev*) mRNA, resulting in decreased levels of 9-kb and 4-kb HIV-1 RNAs in the cytosol (Zhabokritsky et al. 2014). Since overexpression of Rev in the presence of PAP recovered the splicing ratio of HIV-1 RNAs but did not rescue HIV-1 protein expression, it was possible that PAP targeted and depurinated 9-kb and 4-kb RNAs once they were exported out of the nucleus (Zhabokritsky et al. 2014). In my study, I wanted to determine if the 4-kb RNA from which Vif is expressed is targeted by PAP, resulting in decreased Vif protein levels.

Immunoprecipitation of PAP-bound RNAs showed that PAP interacts with Vif mRNA (Figure 8). In addition, Figure 9A shows that PAP decreased the levels of cytosolic Vif mRNA

expressed from the proviral clone pMenv(-) 3-fold relative to cells transfected with pMenv(-) alone. Overexpression of Rev increased the levels of Vif RNA by 2-fold, but did not fully recover it (Figure 9A). Therefore, even in the presence of Rev, when 4-kb mRNA from which Vif is expressed is exported out of the nucleus, Vif mRNA levels are decreased in the presence of PAP. In comparison, Vif protein levels were decreased to undetectable amounts when PAP was present and overexpression of Rev did not change the amount of Vif protein (Figure 9B). The lack of an increase in Vif protein amount when Rev was overexpressed as seen in Figure 9B contradicts the 2-fold increase in the Vif RNA levels. Therefore, although cytosolic levels of Vif RNAs are recovered by the overexpression of Rev, these RNAs are not translated, suggesting that PAP damages them. PAP may be depurinating 2 kb transcripts first, resulting in a lack of Rev protein required for the export of 9 kb and 4 kb transcripts. Therefore, in the absence of Rev, decreased levels of Vif mRNA can be due to nuclear retention. However, since overexpression of Rev did not lead to full recovery of Vif mRNA in the presence of PAP, PAP may also be targeting Vif mRNA directly and depurinating it, resulting in decreased amount of Vif mRNA detected by RT-qPCR.

The 3- fold decrease in Vif RNA levels in the presence of PAP was also shown in H9 lymphocytic cell line which expresses A3G endogenously (Figure 9C). Therefore, H9 lymphocytes, more physiologically relevant cells for HIV-1 infection, supported the trend observed in HEK293T cells, indicating that PAP reduces Vif mRNA levels, present either as an ectopically expressed RNA or from the context of the HIV-1 genome.

4.4 PAP directly depurinates Vif mRNA

Although the ability of PAP to target and depurinate different HIV-1 RNAs has been shown (Zarling et al. 1990, Zhabokritsky et al. 2014), depurination of Vif mRNA has not been demonstrated. Figure 10A and B show that depurination was detected in Vif RNA when expressed from pc-hVif (G5252) clone or the HIV proviral clone (A5222 and C5309). Depurination of RNA substrate leaves an intact ribose-phosphate backbone, but generates a nucleotide missing a purine base. Previous study showed that translating ribosome stalls at apurinic sites, resulting in the inhibition of the synthesis of the full-length protein (Gandhi et al. 2008b). In yeast, stalling of the ribosome at the depurinated site within brome mosaic virus (BMV) RNA3 was correlated with increased degradation of the RNA through the No-go decay (NGD) pathway (Gandhi et al. 2008b). However, the consequence of RNA depurination in mammals remains unclear and it is not known whether stalling of the ribosome at apurinic sites is associated with accelerated degradation in a similar way as observed in yeast.

The depurination sites in Vif RNA expressed from the pMenv(-) proviral clone differed from the depurination site detected in hVif mRNA, perhaps due to differences in mRNA sequences and folding, as the primary sequence in hVif clone was optimized by 26% in this region (Nguyen et al. 2004) and the transcripts vary in size considerably. Vif ORF exists in a context of 4-kb transcript when expressed from the proviral clone compared to only the sequence representing the Vif ORF present in the pc-hVif clone. Therefore, differential folding of the RNAs may alter the structure and therefore identity of the nucleotide base targeted by PAP, implying that structure of the RNA may be important for PAP specificity. Currently, unpublished data from our laboratory suggest that high degree of secondary structure in viral RNAs might be favoured by PAP (Jobst and Hudak). In contrast, analysis of the reported depurinated sites within

BMV, HTLV-1 and HIV-1 RNAs showed no sequence similarity, implying that sequence does not determine the specificity of PAP for viral RNAs (Jobst and Hudak).

4.5 Decreased Vif protein levels in the presence of PAP are correlated with increased A3G levels.

Vif targets A3G for destruction, thereby counteracting its anti-viral activity (Yu et al. 2003, Marin et al. 2003, Mehle et al. 2004, Sheehy et al. 2003, Stopak et al. 2003). PAP inhibited Vif expression when either construct was used, pc-hVif or pMenv(-), indicating that PAP can target Vif in the absence of the other HIV- proteins (Figure 12). In addition, since PAPx did not alter levels of Vif, downregulation by PAP is dependent on its catalytic activity (Figure 12). The loss of Vif protein expression in the presence of PAP can be explained by the depurination detected in Vif RNA expressed from the pc-hVif or pMenv(-) constructs.

To determine the effect of the inhibition of Vif expression by PAP on A3G levels, HeLa and HEK293 cells containing stably integrated A3G gene were used. Data from Figure 13 showed that PAP inhibited Vif expression in these cell lines and rescued cytosolic A3G levels. The rescue of A3G expression detected by western blot was similar to recovery of A3G levels seen in other studies when HIVΔ*vif* mutants were used (Bishop et al. 2008, Sheehy et al. 2003). The degree of inhibition of Vif activity directly affects the ability of A3G to restrict viral propagation. Given that Vif was not detected in PAP-expressing cells and A3G levels were recovered to those of untransfected cells, PAP might be efficient at restricting viral propagation. In addition, the ability of PAP to decrease expression of other HIV-1 proteins is beneficial as it affects multiple steps in the viral life cycle rather than specifically inhibiting Vif action.

In vivo studies showed an inverse correlation between A3G expression levels and HIV-viremia (Jin et al. 2005). Long-term non-progressors (LTNPs) had the highest A3G mRNA levels, followed by HIV-uninfected subjects and progressors (Jin et al. 2005). These studies imply that inhibition of Vif function might significantly reduce HIV-1 virus loads *in vivo* and restrict viral propagation. Therefore, Vif-A3G interaction could be used as a novel target for anti-retroviral therapy. Different strategies have been attempted to either disrupt Vif-A3G interaction or increase A3G levels, as potential anti-HIV therapies. For example, libraries of small molecules have been screened to identify compounds that inhibit Vif-A3G binding, its deaminase activity, extend A3G stability or disrupt the assembly of the E3 ligase complex with A3G and Vif (Cen et al. 2010, Nathans et al. 2008, Matsui et al. 2014, Ali et al. 2012, Zuo et al. 2012). Small molecules that enhanced Vif degradation showed increased A3G encapsidation and hypermutation of HIV-1 DNA (Nathans et al. 2008). Over-expression of A3G has been accomplished by treatment of cells with interferon (Chen et al. 2010). Delivery of vectors containing the A3G gene fused to viral protein Vpr or non-pathogenic variant of Nef showed resistance of the fusion protein to Vif-mediated degradation (Ao et al. 2011, Ao et al. 2008, Green et al. 2009). These strategies have diminished virus production; however, the natural balance between Vif and A3G levels needs to be considered when evaluating potential therapies.

There is growing evidence that HIV-1 uses A3G to promote quasispecies evolution of the virus (Simon et al. 2005, Sadler et al. 2010, Smith 2011, Wood et al. 2009). Perhaps incomplete inhibition of Vif would maintain A3G at low levels that would serve to create new, potentially more fit, variants of the viral genome. There is evidence that cytidine deamination provides a source for viral diversification and facilitate HIV-1 escape from immunological and pharmaceutical inhibition (Simon et al. 2005, Wood at al. 2009). Many drug-resistance mutations

were shown to reside in A3G hotspots, suggesting that mutations introduced by A3G give rise to HIV-1 variants resistant to common anti-HIV drugs (Berkhout and deRonde 2004). In addition, mutations in cytotoxic T cell (CTL) epitopes were found in A3G hotspots (Wood et al. 2009). CTLs play an important role in adaptive immunity in elimination of virally infected cells and mutations in CTL epitopes were shown affect activation of these cells (Borrow et al. 1997). Therefore, this alternate view that A3G can promote virus fitness must be carefully considered when designing drugs that inhibit Vif function and provides a challenge when designing therapeutic approaches aimed at disturbing the Vif-A3G interaction.

4.6 PAP decreases infectivity of HIV-1 virions and reduces levels of integrated HIV-1 proviral DNA in infected cells.

Previous studies showed that PAP decreases HIV-1 particle release from HEK293T cells by 450-fold (Mansouri et al. 2012). However, HIV-1 virions released from PAP-expressing cells were 7-fold more infectious, which was attributed to the activation of ERK1/2 MAPK pathway and subsequent phosphorylation of p17 matrix protein (Mansouri et al. 2012). The increase in infectivity of HIV-1 virions in the presence of PAP was compensated by the significant reduction in virus particle release, resulting in overall decrease in virus production upon *de novo* infection of cells over 21-day period (Mansouri et al. 2012). Activation of ERK1/2 MAPK signalling pathway is thought to be triggered by depurination of 28S rRNA; PAP and other RIPs have been shown to induce a ribotoxic stress response following the damage to the ribosome (Iordanov et al. 1997). Although apoptosis is often the end-result of ribotoxic stress response (Iordanov et al. 1997), the activation of c-Jun NH_2-terminal kinase (JNK) when PAP was transiently expressed in HEK293T cells did not result in cell death (Chan Tung et al. 2008). Overall, studies conducted in

HEK293T cells showed that PAP increases infectivity of HIV-1 virions by activating MAPK pathways (Chan Tung et al. 2008, Mansouri et al. 2012). However, these studies were conducted in a cell line that does not express A3G. Since A3G significantly reduces infectivity of HIV-1 virions in the absence of functional Vif protein, I investigated the effect of PAP expression in HeLa-A3G cells on HIV-1 particle release and infectivity.

Transient expression of PAP in HeLa-A3G cells reduced HIV-1 particle release in concentration dependent manner (Figure 14). Approximately 100-fold reduction was observed at the highest concentration of PAP tested (Figure 14). This concentration of PAP was shown to not cause change in cell viability (Figure 7B). The difference in the reduction of HIV-1 particle release observed in HeLa-A3G cells and reported in HEK293T cells (Mansouri et al. 2012) could be due to differences between cells lines and transient tranfection settings, including variable amount of DNA vectors used and transfection efficiency.

To determine the effect of PAP on infectivity of HIV-1 virions released from HeLa-A3G cells, HIV-1 particles pseudotyped with VSV-G were used to infect 1G5 cells, a derivative of Jurkat cell line stably expressing a luciferase reporter gene downstream of HIV-1 long terminal repeat (LTR). Activation of the LTR requires efficient expression of HIV-1 regulatory protein Tat which is the primary regulator of HIV-1 transcription (Berkhout et al. 1989). Therefore, successful infection and expression of HIV-1 RNAs and proteins are required for Luciferase expression. Virions from PAP-expressing cells were approximately 11-fold less infectious, as indicated by decreased luciferase activity, compared to virions from PAPx or pcDNA3 cells (Figure 15A). Other studies showed 10-1000 fold decrease in infectivity of HIV-1Δ*vif* virions (Strebel 1987, Mangeat et al. 2003, Mariani et al. 2003, Kao et al. 2003, Sheehy et al. 2003, Miyagi et al. 2007). This wide range of reported reduction in viral infectivity in the absence of

Vif could be due to use of different cell lines expressing variable levels of A3G, use of transient transfection to express A3G exogenously, different proviral clones and experimental procedures.

Overall, PAP expression lowered production of infectious HIV-1 particles; 100-fold reduction in release of viral particles and 10-fold decrease in infectivity of virions were shown. It is likely that PAP also activates MAPK pathways in HeLa cells, although this has not been demonstrated and requires further investigation. If PAP induces phosporylation of p17 matrix protein in HeLa cells in a similar way as observed in HEK293T cells, then the activity of A3G outweights the effect of PAP on MAPK pathway activation and its subsequent impact on infectivity. However, activation of the MAPK pathway and phosphorylation of p17 matrix protein upon transfection of PAP into HeLa cells not expressing A3G should be first evaluated before drawing conclusions about the contradictory results observed between the two cell lines.

The 100-fold decline in virus particle release from PAP-expressing cells did not provide enough material to confirm the presence of A3G in released HIV-1 particles. Therefore, to test the activity of A3G, I wanted to determine the levels of integrated HIV-1 DNA in target 1G5 cells since A3G reduces reverse transcript accumulation and integration of proviral DNA (von Schwedler et al. 1993, Goncalves et al. 1996, Mariani et al. 2003, Mangeat et al. 2003). Expression of PAP in producer HeLa-A3G cells significantly reduced the amount of integrated proviral HIV-1 DNA in target 1G5 cells (Figure 15B). Other studies showed 5-50 fold reduction in integration efficiency of HIV-1Δ*vif* viruses (Mangeat et al. 2003, Mariani et al. 2003, Luo et al. 2007). The absence of HIV-1 proviral DNA in 1G5 cells did not allow me to investigate hypermutation status. It would be of interest to determine the reduction in integrated HIV-1 DNA more quantitatively by performing qPCR and using primers than span different regions of

HIV-1 DNA to confirm the results and analyze sequences to determine if hypermutation occurs when a gradient of PAP is transfected into producer cells.

4.7 Anti-HIV-1 activity of PAP and its application

In my study, I showed that PAP reduced HIV-1 particle production and the released virions were less infectious. This effect on infectivity was attributed to inhibition of Vif expression by PAP and its subsequent impact on A3G. Therefore, I propose a model in which increased A3G levels in the presence of PAP reduce the release of infectious viral particles and inhibit further viral propagation (Figure 16). Previous studies performed in our lab showed that PAP depurinates other HIV-1 RNAs, including Rev RNA, thereby inhibiting different steps of the viral life cycle (Zhabokritsky et al. 2014). Inhibition of Rev activity resulted in nuclear retention of 9-kb and 4-kb RNAs (Zhabokritsky et al. 2014). The lack of recovery of HIV-1 protein expression when Rev was overexpressed suggested that when exported out of the nucleus, 9-kb and 4-kb HIV-1 RNAs can be templates for depurination. Because of its ability to inhibit the expression of multiple viral proteins simultaneously and decrease the release of infectious virions, PAP could act as a potential therapeutic agent against HIV-1.

Current treatments involve administration of combination of drugs, each targeting different steps of the HIV-1 life cycle to minimize the chance of drug resistance arising due to the highly mutagenic nature of HIV-1. Some of the drugs currently used include nucleoside and non-nucleoside analogs that inhibit reverse transcriptase and protease (Barre-Sinoussi et al. 2013, Siliciano et al. 2013). Per round of replication, HIV-1 RT introduces on average 5-10 mutations in HIV-1 genome (Preston et al. 1988). Analyses of the misincorporated bases showed

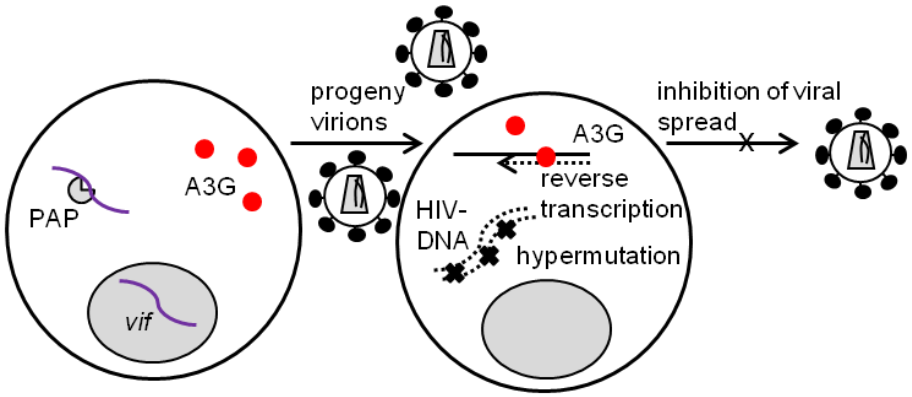

Figure 16. Model for inhibition of Vif by PAP and its impact on A3G-mediated defense. PAP depurinates Vif RNA, which inhibits its translation. Decreased levels of Vif correlate with increased levels of A3G. A3G gets incorporated into budding viral particles and upon infection of susceptible cells, the deaminase enzyme decreases accumulation of reverse transcripts and induces hypermutation of HIV-1 DNA. Therefore, inhibition of Vif by PAP upregulates levels of A3G and limits viral spread.

a preference of the RT enzyme for purine to purine substitutions or pyrimidine to pyrimidine substitutions (Preston et al. 1988). Since PAP can target different HIV-1 RNAs, the ability of the virus to develop resistance and escape the anti-viral activity of PAP would be minimized compared to drugs relying on inhibiting the activity of one specific viral enzyme. In addition, the very A-rich nature of the HIV genome (35% A) (van der Kuyl and Berkhout 2012), combined with the RT nucleotide misincorporation bias would minimize the emergence of PAP resistance.

4.8 Conclusions and future directions

Inhibition of Vif by PAP could explain the observed reduction in infectivity of HIV-1 virions; however it does not explain the overall decrease in virus particle release, as the absence of Vif does not affect the amount of viral particles produced. Previous study showing inhibition of Rev activity suggested other HIV-1 RNAs can be targeted for depurination, as overexpression of Rev restored the 9-kb and 4-kb mRNAs to the cytosol, but did not recover viral protein expression (Zhabokritsky et al. 2014). Therefore, primer extension to detect depurinations in *gag* and *pol* ORFs should be performed to determine if the 9-kb and 4-kb RNAs can also be targeted by PAP.

In addition, knowing how these RNAs are selected as targets for depurination would aid in our understanding of the antiviral activity of PAP. Previously, it has been shown that PAP is located in the cytosol in HEK293T cells (Mansouri et al. 2009); however, it is unknown whether PAP localizes to specific cytosolic foci such as P-bodies that are associated with viral infections. It would be interesting to see if HIV-1 RNAs and PAP co-localize in specific sub-cellular compartments. In addition, little is known about what cellular proteins interact with PAP. Binding of PAP to host factors could allow recruitment of PAP to viral RNAs. Therefore,

performing co-immunoprecipitation experiments to identify binding interactions could reveal potential cellular proteins involved in PAP anti-viral activity.

Next, my data show that transient expression of PAP decreases infectivity of HIV-1 particles which was attributed to increased A3G levels. In order to further support this, infectivity studies with HeLa cells not expressing A3G should be performed. Determining the infectivity of HIV-1 virions released from HeLa cells would also test whether in the absence of A3G, the infectivity of viral particles is increased due to activation of MAPK pathways as seen in HEK293T cells (Mansouri et al. 2012). In addition, studies in other cell lines, including T-cell lines endogenously expressing A3G, would be beneficial as it would provide more suitable model to study HIV-1 infection. Therefore, multiple factors contribute to the observed infectivity of HIV-1 virions in the presence of PAP and differential expression of host factors in cell lines can cause variable results.

In the current study, I looked at transient expression of PAP and its effect on A3G-mediated immune defense. It would be beneficial to look at the effect of PAP in a producer cell line expressing A3G on virus propagation over a longer time period. Determination of virus production over a longer time period could show if PAP is efficient at restricting production of infectious viruses. In addition, long-term study could also reveal whether PAP resistance is acquired with time and therefore determine the effectiveness of PAP as a biotherapeutic agent against HIV-1.

5. REFERENCES

Alce TM and Popik W. 2004. APOBEC3G is incorporated into virus-like particles by a direct interaction with HIV-1 Gag nucleocapsid protein. *J Biol Chem* **279**(33): 34083-6.

Ali A, Wang J, Nathans RS, Cao H, Sharova N, Stevenson M, Rana TM. 2012. Synthesis and structure-activity relationship studies of HIV-1 virion infectivity factor (Vif) inhibitors that block viral replication. *Chem Med Chem* **7**(7): 1217-29.

Arhel N. 2010. Revisiting HIV-1 uncoating. *Retrovirol* **7**:96-106.

Arias JF, Koyama T, Kinomoto M, Tokunaga K. 2012. Retroelements versus APOBEC3 family members: No great escape from the magnificent seven. *Front Microbiol* **3**:275. doi: 10.3389/fmicb.2012.00275

Aron GM and Irvin JD. 1980. Inhibition of herpes simplex virus multiplication by the pokeweed antiviral protein. *Antimicrob Agents Chemother* **17**(6): 1032-3.

Ao Z, Yu Z, Wang L, Zheng Y, Yao X. 2008. Vpr14-88-Apobec3G Fusion Protein Is Efficiently Incorporated into Vif-Positive HIV-1 Particles and Inhibits Viral Infection. *PLoS ONE* 3(4): e1995

Ao Z, Wang X, Bello A, Jayappa KD, Yu Z, Fowke K, He X, Chen X, Li J, Kobinger G, Yao X. 2011. Characterization of anti-HIV activity mediated by R88-APOBEC3G mutant fusion proteins in CD4+ T cells, peripheral blood mononuclear cells, and macrophages. *Hum Gene Ther* **22**(10): 1225-37.

Arakawa H, Hauschild J, Buerstedde JM. 2002. Requirement of the activation-induced deaminase (AID) gene for immunoglobulin gene conversion. *Science* **295**(5558): 1301-6.

Barré-Sinoussi F, Chermann JC, Rey F, Nugeyre MT, Chamaret S, Gruest J, Dauguet C, Axler-Blin C, Vézinet-Brun F, Rouzioux C, Rozenbaum W, Montagnier L. 1983. Isolation of a T-lymphotropic retrovirus from a patient at risk for acquired immune deficiency syndrome (AIDS). *Science* **220**(4599): 868-71.

Barrè-Sinoussi F, Ross AL, Delfraissy J. 2013. Past, present and future: 30 years of HIV research. *Nature Rev Microbiol* **11**: 877-83.

Berkhout B, Silverman RH, Jeang KT. 1989. Tat trans-activates the human immunodeficiency virus through a nascent RNA target. *Cell* **59**(2): 273-82.

Berkhout B and de Ronde A. 2004. APOBEC3G versus reverse transcriptase in the generation of HIV-1 drug-resistance mutations. *AIDS* **18**(13): 1861-3.

Bishop KN, Holmes RK, Sheehy AM, Davidson NO, Cho SJ, Malim MH. 2004. Cytidine deamination of retroviral DNA by diverse APOBEC proteins. *Curr Biol* **14**(15): 1392-6.

Bishop KN, Verma M, Kim EY, Wolinsky SM, Malim MH. 2008. APOBEC3G inhibits elongation of HIV-1 reverse transcripts. *PLoS Pathog* **4**(12):e1000231.

Bogerd HP, Doehle BP, Wiegand HL, Cullen BR. 2004. A single amino acid difference in the host APOBEC3G protein controls the primate species specificity of HIV type 1 virion infectivity factor. *Proc Natl Acad Sci U S A.* **101**(11):3770-4.

Borrow P, Lewicki A, Wei X, Horwitz MS, Peffer N, Meyers H, Nelson JA, Gairin JE, Hahn BH, Oldstone MBA, Shaw GM. 1997. Antiviral pressure exerted by HIV-l-specific cytotoxic T lymphocytes (CTLs) during primary infection demonstrated by rapid selection of CTL escape virus. *Nature Med* **3**: 205-11.

Britan-Rosich E, Nowarski R, Kotler M. 2011. Multifaceted counter-APOBEC3G mechanisms employed by HIV-1 Vif. *J Mol Biol* **410**(5): 1065-76.

Cen S, Guo F, Niu M, Saadatmand J, Deflassieux J, Kleiman L. 2004. The interaction between HIV-1 Gag and APOBEC3G. *J Biol Chem* **279**(32): 33177-84.

Cen S, Peng ZG, Li XY, Li ZR, Ma J, Wang YM, Fan B, You XF, Wang YP, Liu F, Shao RG, Zhao LX, Yu L, Jiang JD. 2010. Small molecular compounds inhibit HIV-1 replication through specifically stabilizing APOBEC3G. *J Biol Chem* **285**(22): 16546-52.

Chan Tung, K. W., Mansouri, S., and Hudak, K. A. (2008) Expression of pokeweed antiviral protein in mammalian cells activates c-Jun NH2-terminal kinase without causing apoptosis. *Int. J. Biochem. Cell Biol.* **40**, 2452–2461

Chen SH, Habib G, Yang CY, Gu ZW, Lee BR, Weng SA, Silberman SR, Cai SJ, Deslypere JP, Rosseneu M. 1987. Apolipoprotein B-48 is the product of a messenger RNA with an organ-specific in-frame stop codon. *Science* **238**(4825):363-6.

Chen H, Wang LW, Huang YQ, Gong ZJ. 2010. Interferon-alpha induces high expression of APOBEC3G and STAT-1 in vitro and in vivo. *Int J Mol Sci* **11**(9): 3501-12.

Chiu YL, Soros VB, Kreisberg JF, Stopak K, Yonemoto W, Greene WC. 2005. Cellular APOBEC3G restricts HIV-1 infection in resting CD4+ T cells. *Nature* **435**(7038): 108-14.

Cobos Jiménez V, Booiman T, de Taeye SW, van Dort KA, Rits MA, Hamann J, Kootstra NA. 2012. Differential expression of HIV-1 interfering factors in monocyte-derived macrophages stimulated with polarizing cytokines or interferons. *Sci Rep* **2**:763. doi: 10.1038/srep00763.

Cohen MS, Shaw GM, McMichael AJ, Haynes BF. 2011. Acute HIV-1 Infection. *N Engl J Med* **364**(20): 1943-54.

Conticello SG, Harris RS, Neuberger MS. 2003. The Vif protein of HIV triggers degradation of the human antiretroviral DNA deaminase APOBEC3G. *Curr Biol* **13**(22): 2009-13.

Cullen BR. 1991. Regulation of HIV-1 expression. *FASEB J* **5**(10): 2361-8.

Cullen BR. 2006. Role and mechanism of action of the APOBEC3 family of antiretroviral resistance factors. *J of Virol* **80**(3): 1067-76.

Desimmie BA, Delviks-Frankenberrry KA, Burdick RC, Qi D, Izumi T, Pathak VK. 2014. Multiple APOBEC3 restriction factors for HIV-1 and one Vif to rule them all. *J Mol Biol* **426**(6): 1220-45.

Duggar BM and Armstrong JK. 1925. The effect of treating virus of tobacco mosaic with juice of various plants. *Ann Mol Bot Gard* **12**: 359-65.

Endo Y, Mitsui K, Motizuki M, Tsurugi K. 1987. The mechanism of action of ricin and related toxic lectins on eukaryotic ribosomes. The site and the characteristics of the modification in 28 S ribosomal RNA caused by the toxins. *J Biol Chem* **262**(12): 5908-12.

Erice A, Balfour HH, Myers DE, Leske VL, Sannerud KJ, Kuebelbeck V, Irvin JD, and Uckun FM. 1993. Anti-human immunodeficiency virus type 1 activity of an anti-CD4 immunoconjugate containing pokeweed antiviral protein. *Antimicrob Agents Chemother* **37**(4): 835-8.

Esnault C, Millet J, Schwartz O, Heidmann T. 2006. Dual inhibitory effects of APOBEC family proteins on retrotransposition of mammalian endogenous retroviruses. *Nucleic Acids Res* **34**(5): 1522-31.

Etard C, Roostalu U, Strähle U. 2010. Lack of Apobec2-related proteins causes a dystrophic muscle phenotype in zebrafish embryos. *J Cell Biol* **189**(3): 527-39.

Eyzaguirre LM, Charurat M, Redfield RR, Blattner WA, Carr JK, Sajadi MM. 2013. Elevated hypermutation levels in HIV-1 natural viral suppressors. *Virol* **443**(2): 306-12.

Fan J, Ma G, Nosaka K, Tanabe J, Satou Y, Koito A, Wain-Hobson S, Vartanian JP, Matsuoka M. 2010. APOBEC3G generates nonsense mutations in human T-cell leukemia virus type 1 proviral genomes in vivo. *J Virol* **84**(14): 7278-87.

Foà-Tomasi L, Campadelli-Fiume G, Barbieri L, Stirpe F. 1982. Effect of ribosome-inactivating proteins on virus-infected cells. Inhibition of virus multiplication and of protein synthesis. *Arch Virol* ***71***(4): 323-32.

Gabuzda DH, Lawrence K, Langhoff E, Terwilliger E, Dorfman T, Haseltine WA, Sodroski J. 1992. Role of vif in replication of human immunodeficiency virus type 1 in CD4+ T lymphocytes. *J Virol* **66**(11): 6489-95.

Gandhi SK, Siliciano JD, Bailey JR, Siliciano RF, Blankson JN. 2008a. Role of APOBEC3G/F-mediated hypermutation in the control of human immunodeficiency virus type 1 in elite suppressors. *J Virol* **82**(6): 3125-30.

Gandhi, R., Manzoor, M., and Hudak, K. A. 2008b. Depurination of Brome mosaic virus RNA3 in vivo results in translation-dependent accelerated degradation of the viral RNA. *J. Biol. Chem.* **283**: 32218–32228.

Gessner SL and Irvin JD. 1980. Inhibition of elongation factor 2-dependent translocation by the pokeweed antiviral protein and ricin. *J Biol Chem* **255**(8): 3251-3.

Girbes T, Ferreras J, Arias F. 2004. Description, distribution, activity and phylogenetic relationship of ribosome-inactivating proteins in plants, fungi and bacteria. *Mini Rev Med Chem* **4**(5): 461-76

Goncalves J, Korin Y, Zack J, Gabuzda D. 1996. Role of Vif in human immunodeficiency virus type 1 reverse transcription. *J Virol* **70**(12): 8701-9.

Gottfredsson M and Bohjanen PR. 1997. Human immunodeficiency virus type I as a target for gene therapy. *Front Biosci* **15**(2): d619-34.

Green LA, Liu Y, He JJ. 2009. Inhibition of HIV-1 infection and replication by enhancing viral incorporation of innate anti-HIV-1 protein A3G: a non-pathogenic Nef mutant-based anti-HIV strategy. *J Biol Chem* **284**(20): 13363-72.

Guo F, Cen S, Niu M, Yang Y, Gorelick RJ, Kleiman L. 2007. The interaction of APOBEC3G with human immunodeficiency virus type 1 nucleocapsid inhibits tRNA3Lys annealing to viral RNA. *J Virol* **81**(20):11322-31.

Hamilton CE, Papavasiliou FN, Rosenberg BR. 2010. Diverse functions for DNA and RNA editing in the immune system. *RNA Biol* **7**(2): 220-8.

Harris RS, Bishop KN, Sheehy AM, Craig HM, Petersen-Mahrt SK, Watt IN, Neuberger MS, Malim MH. 2003. DNA deamination mediates innate immunity to retroviral infection. *Cell* **113**(6): 803-9.

Harris RS, Gross JD, Krogan NJ. 2011. Vif hijacks CBF-β to degrade APOBEC3G and promote HIV-1 infection. *Nature* **481**(7381): 371-5.

Huang PL, Sun Y, Chen HC, Kung HF, Lee-Huang S. 1999. Proteolytic fragments of anti-HIV and anti-tumor proteins MAP30 and GAP31 are biologically active. *Biochem Biophys Res Commun* **262**(3): 615-23.

Hultquist JF, Lengyel JA, Refsland EW, LaRue RS, Lackey L, Brown WL, Harris RS. 2011. Human and rhesus APOBEC3D, APOBEC3F, APOBEC3G, and APOBEC3H demonstrate a conserved capacity to restrict Vif-deficient HIV-1. *J Virol* **85**(21): 11220-34.

Hur Y, Hwang DJ, Zoubenko O, Coetzer C, Uckun FM, Tumer NE. 1995. Isolation and characterization of pokeweed antiviral protein mutations in Saccharomyces cerevisiae: identification of residues important for toxicity. *Proc Natl Acad Sci U S A* **92**(18): 8448-52.

Huthoff H and Malim MH. 2007. Identification of amino acid residues in APOBEC3G required for regulation by human immunodeficiency virus type 1 Vif and Virion encapsidation. *J Virol* **81**(8): 3807-15.

Iordanov MS, Pribnow D, Magun JL, Dinh TH, Pearson JA, Chen SL, Magun BE. 1997. Ribotoxic stress response: activation of the stress-activated protein kinase JNK1 by inhibitors of the peptidyl transferase reaction and by sequence-specific RNA damage to the alpha-sarcin/ricin loop in the 28S rRNA. *Mol Cell Biol* **17**(6): 3373-81.

Iwatani Y, Chan DS, Wang F, Maynard KS, Sugiura W, Gronenborn AM, Rouzina I, Williams MC, Musier-Forsyth K, Levin JG. 2007. Deaminase-independent inhibition of HIV-1 reverse transcription by APOBEC3G. *Nucleic Acids Res* **35**(21): 7096-108.

Jarmuz A, Chester A, Bayliss J, Gisbourne J, Dunham I, Scott J, Navaratnam N. 2002. An anthropoid-specific locus of orphan C to U RNA-editing enzymes on chromosome 22. *Genomics* **79**(3): 285-96.

Jin X, Brooks A, Chen H, Bennett R, Reichman R, Smith H. 2005. APOBEC3G/CEM15 (hA3G) mRNA levels associate inversely with human immunodeficiency virus viremia. *J Virol* **79**(17): 11513-6.

Kao S, Khan MA, Miyagi E, Plishka R, Buckler-White A, Strebel K. 2003. The human immunodeficiency virus type 1 Vif protein reduces intracellular expression and inhibits packaging of APOBEC3G (CEM15), a cellular inhibitor of virus infectivity. *J Virol* **77**(21): 11398-407.

Kao S, Goila-Gaur R, Miyagi E, Khan MA, Opi S, Takeuchi H, Strebel K. 2007. Production of infectious virus and degradation of APOBEC3G are separable functional properties of human immunodeficiency virus type 1 Vif. *Virology* **369**(2): 329-39.

Karran RA and Hudak KA. 2008. Depurination within the intergenic region of Brome mosaic virus RNA3 inhibits viral replication in vitro and *in vivo*. *Nucleic Acids Res* **36**(22): 7230-9.

Khan MA, Kao S, Miyagi E, Takeuchi H, Goila-Gaur R, Opi S, Gipson CL, Parslow TG, Ly H, Strebel K. 2005. Viral RNA is required for the association of APOBEC3G with human immunodeficiency virus type 1 nucleoprotein complexes. *J Virol* **79**(9): 5870-4.

Koning FA, Newman EN, Kim EY, Kunstman KJ, Wolinsky SM, Malim MH. 2009. Defining APOBEC3 expression patterns in human tissues and hematopoietic cell subsets. *J Virol* **83**(18): 9474-85.

Kourteva Y, De Pasquale M, Allos T, McMunn C, D'Aquila RT. 2012. APOBEC3G expression and hypermutation are inversely associated with human immunodeficiency virus type 1 (HIV-1) burden in vivo. *Virol* **430**(1): 1-9.

Kozak SL, Marin M, Rose KM, Bystrom C, Kabat D. 2006. The anti-HIV-1 editing enzyme APOBEC3G binds HIV-1 RNA and messenger RNAs that shuttle between polysomes and stress granules. *J Biol Chem* **281**(39): 29105-19.

Langlois MA and Neuberger MS. 2008. Human APOBEC3G can restrict retroviral infection in avian cells and acts independently of both UNG and SMUG1. *J Virol* **82**(9): 4660-4.

Lecossier D, Bouchonnet F, Clavel F, Hance AJ. 2003. Hypermutation of HIV-1 DNA in the absence of the Vif protein. *Science* **300**(5622): 1112.

Lee-Huang S, Kung HF, Huang PL, Bourinbaiar AS, Morell JL, Brown JH, Huang PL, Tsai WP, Chen AY, Huang HI. 1994. Human immunodeficiency virus type 1 (HIV-1) inhibition, DNA-binding, RNA-binding, and ribosome inactivation activities in the N-terminal segments of the plant anti-HIV protein GAP31. *Proc Natl Acad Sci U S A* **91**(25): 12208-12.

Levy JA. 1993. Pathogenesis of human immunodeficiency virus infection. *Microbiol Rev* **57**(1): 183-9.

Li XP, Baricevic M, Saidasan H, Tumer NE. 2007. Ribosome depurination is not sufficient for ricin-mediated cell death in Saccharomyces cerevisiae. *Infect Immun* **5**(1): 417-28.

Liddament MT, Brown WL, Schumacher AJ, Harris RS. 2004. APOBEC3F properties and hypermutation preferences indicate activity against HIV-1 in vivo. *Curr Biol* **14**(15): 1385-91.

Lin Q, Chen ZC, Antoniw JF, White RF. 1991. Isolation and characterization of a cDNA clone encoding the anti-viral protein from Phytolacca americana. *Plant Mol Biol* **17**(4): 609-14.

Luo K, Liu B, Xiao Z, Yu Y, Yu X, Gorelick R, Yu XF. 2004. Amino-terminal region of the human immunodeficiency virus type 1 nucleocapsid is required for human APOBEC3G packaging. *J Virol* **78**(21): 11842-52.

Luo K, Wang T, Liu B, Tian C, Xiao Z, Kappes J, Yu XF. 2007. Cytidine deaminases APOBEC3G and APOBEC3F interact with human immunodeficiency virus type 1 integrase and inhibit proviral DNA formation. *J Virol* **81**(13): 7238-48.

Ma J, Li X, Xu J, Zhang Q, Liu Z, Jia P, Zhou J, Guo F, You X, Yu L, Zhao L, Jiang J, Cen S. 2011. The cellular source for APOBEC3G's incorporation into HIV-1. *Retrovirol* **8**:2. doi: 10.1186/1742-4690-8-2.

Malim MH and Bieniasz PD. 2012. HIV Restriction Factors and Mechanisms of Evasion. Cold *Spring Harb Perspect Med* **2**(5): a006940. doi: 10.1101/cshperspect.a006940.

Mangeat B, Turelli P, Caron G, Friedli M, Perrin L, Trono D. 2003. Broad antiretroviral defence by human APOBEC3G through lethal editing of nascent reverse transcripts. *Nature* **424** (6944): 99-103.

Mangeat B, Turelli P, Liao S, Trono D. 2004. A single amino acid determinant governs the species-specific sensitivity of APOBEC3G to Vif action. *J Biol Chem* **279**(15): 14481-3.

Mansouri S, Choudhary G, Sarzala PM, Ratner L, Hudak KA. 2009. Suppression of human T-cell leukemia virus I gene expression by pokeweed antiviral protein. *J Biol Chem* **284**(45): 31453-62.

Mansouri S, Kutky M, Hudak KA. 2012. Pokeweed antiviral protein increases HIV-1 particle infectivity by activating the cellular mitogen activated protein kinase pathway. *PLoS One* **7**(5): e35369 doi: 10.1371/journal.pone.0036369

Marin M, Rose KM, Kozak SL, Kabat D. 2003. HIV-1 Vif protein binds the editing enzyme APOBEC3G and induces its degradation. *Nat Med* **9(**11): 1398-403.

Mariani R, Chen D, Schröfelbauer B, Navarro F, König R, Bollman B, Münk C, Nymark-McMahon H, Landau NR. 2003. Species-specific exclusion of APOBEC3G from HIV-1 virions by Vif. *Cell* **114**(1): 21-31.

Matsui M, Shindo K, Izumi T, Io K, Shinohara M, Komano J, Kobayashi M, Kadowaki N, Harris RS, Takaori-Kondo A. 2014. Small molecules that inhibit Vif-induced degradation of APOBEC3G. *Virol J* **11**:122. doi: 10.1186/1743-422X-11-122.

Mbisa JL, Barr R, Thomas JA, Vandegraaff N, Dorweiler IJ, Svarovskaia ES, Brown WL, Mansky LM, Gorelick RJ, Harris RS, Engelman A, Pathak VK. 2007. Human immunodeficiency virus type 1 cDNAs produced in the presence of APOBEC3G exhibit defects in plus-strand DNA transfer and integration. *J Virol* **81**(13): 7099-110

Mehle A, Strack B, Ancuta P, Zhang C, McPike M, Gabuzda D. 2004. Vif overcomes the innate antiviral activity of APOBEC3G by promoting its degradation in the ubiquitin-proteasome pathway. *J Biol Chem* **279**(9): 7792-8.

Mercenne G, Bernacchi S, Richer D, Bec D, Henriet S, Paillart J,Marquet R. 2003. HIV-1 Vif binds to APOBEC3G mRNA and inhibits its translation. *Nucleic Acids Res* **38**(2): 633-46.

Merson MH, O'Malley J, Serwadda D, Apisuk C. 2008. The history and challenge of HIV prevention. *Lancet* **372**: 475–88.

Miyagi E, Opi S, Takeuchi H, Khan M, Goila-Gaur R, Kao S, Strebel K. 2007. Enzymatically active APOBEC3G is required for efficient inhibition of human immunodeficiency virus type 1. *J Virol* **81**(24): 13346-53.

Monajemi M, Woodworth CF, Benkaroun J, Grant M, Larijani M. 2012. Emerging complexities of APOBEC3G action on immunity and viral fitness during HIV infection and treatment. *Retrovirol* **9**:35 doi: 10.1186/1742-4690-9-35.

Montanaro L, Sperti S, Mattioli A, Testoni G, Stirpe F. 1975. Inhibition by ricin of protein synthesis in vitro. Inhibition of the binding of elongation factor 2 and of adenosine diphosphate-ribosylated elongation factor 2 to ribosomes. *Biochem J* **146**(1):127-31.

Monzingo AF, Collins EJ, Ernst SR, Irvin JD, Robertus JD. 1993. The 2.5 A structure of pokeweed antiviral protein. *J Mol Biol* **233**(4): 705-15.

Muramatsu M, Sankaranand VS, Anant S, Sugai M, Kinoshita K, Davidson NO, Honjo T. 1999. Specific expression of activation-induced cytidine deaminase (AID), a novel member of the RNA-editing deaminase family in germinal center B cells. *J Biol Chem* **274**(26): 18470-6.

Muramatsu M, Kinoshita K, Fagarasan S, Yamada S, Shinkai Y, Honjo T. 2000. Class switch recombination and hypermutation require activation-induced cytidine deaminase (AID), a potential RNA editing enzyme. *Cell* **102**(5): 553-63.

Narayanan S, Surendranath K, Bora N, Surolia A, Karande AA. 2005. Ribosome inactivating proteins and apoptosis. *FEBS Lett* **579**(6): 1324-31.

Nathans R, Cao H, Sharova N, Ali A, Sharkey M, Stranska R, Stevenson M, Rana TM. 2008. Small-molecule inhibition of HIV-1 Vif. *Nat Biotechnol* **26**(10): 1187-92.

Navaratnam N, Morrison JR, Bhattacharya S, Patel D, Funahashi T, Giannoni F, Teng BB, Davidson NO, Scott J. 1993. The p27 catalytic subunit of the apolipoprotein B mRNA editing enzyme is a cytidine deaminase. *J Biol Chem* **268**(28): 20709-12.

Newman EN, Holmes RK, Craig HM, Klein KC, Lingappa JR, Malim MH, Sheehy AM. 2005. Antiviral function of APOBEC3G can be dissociated from cytidine deaminase activity. *Curr Biol* **15**(2): 166-70.

Nguyen KL, llano M, Akari H, Miyagi E, Poeschla EM, Strebel K, Bour S. 2004. Codon optimization of the HIV-1 vpu and vif genes stabilizes their mRNA and allows for highly efficient Rev-independent expression. *Virology* **319(**2): 163-75.

Nielsen K, and Boston RS. 2001. Ribosome-inactivating proteins: a plant respective. *Annu Rev Plant Physiol Plant Mol Biol* **52***: 785-816.*

Nilsson L and Nygard O. 1986. The mechanism of the protein-synthesis elongation cycle in eukaryotes. Effect of ricin on the ribosomal interaction with elongation factors. *Eur J Biochem* **161**: 111–117.

Opi S, Kao S, Goila-Gaur R, Khan MA, Miyagi E, Takeuchi H, Strebel K. 2007. Human immunodeficiency virus type 1 Vif inhibits packaging and antiviral activity of a degradation-resistant APOBEC3G variant. *J Virol* **81**(15): 8236-46.

Passaes CP and Sáez-Cirión A. 2014. HIV cure research: advances and prospects. Virol **454-455**: 340-52.

Peng G, Greenwell-Wild T, Nares S, Jin W, Lei KJ, Rangel ZG, Munson PJ, Wahl SM. 2007. Myeloid differentiation and susceptibility to HIV-1 are linked to APOBEC3 expression. *Blood* **110**(1): 393-400.

Peumans WJ, Hao Q, Van Damme EJ. 2001. Ribosome-inactivating proteins from plants: more than RNA N-glycosidases? *FASEB J* **15**(9): 1493-506.

Pollar VW and Malim MH. 1998. The HIV-1 Rev protein. *Annu Rev Microbiol* **52**:491-32.

Preston BD, Poiesz BJ, Loeb LA. 1988. Fidelity of HIV-1 reverse transcriptase. *Science* **242**(4882): 1168-71.

Prochnow C, Bransteitter R, Klein MG, Goodman MF, Chen XS. 2007. The APOBEC-2 crystal structure and functional implications for the deaminase AID. *Nature* **445**(7126): 447-51.

Purcell DF and Martin MA. 1993. Alternative splicing of human immunodeficiency virus type 1 mRNA modulates viral protein expression, replication, and infectivity. *J Virol* **67**(11): 6365-78.

Rajamohan F, Venkatachalam TK, Irvin JD, Uckun FM. 1999. Pokeweed antiviral protein isoforms PAP-I, PAP-II, and PAP-III depurinate RNA of human immunodeficiency virus (HIV)-1. *Biochem Biophys Res Commun* **260**(2): 453-8.

Ready MP, Brown DT, Robertus JD. 1986. Extracellular localization of pokeweed antiviral protein. *Proc Natl Acad Sci U S A* **83**(14): 5053-6.

Refsland EW, Stenglein MD, Shindo K, Albin JS, Brown WL, Harris RS. 2010. Quantitative profiling of the full APOBEC3 mRNA repertoire in lymphocytes and tissues: implications for HIV-1 restriction. *Nucleic Acids Res* **38**(13): 4274-84.

Rogozin IB, Basu MK, Jordan IK, Pavlov YI, Koonin EV. 2005. APOBEC4, a new member of the AID/APOBEC family of polynucleotide (deoxy)cytidine deaminases predicted by computational analysis. *Cell Cycle* **4**(9): 1281-5.

Rose KM, Marin M, Kozak SL, Kabat D. 2005. Regulated production and anti-HIV type 1 activities of cytidine deaminases APOBEC3B, 3F, and 3G. *AIDS Res Hum Retroviruses* **21**(7): 611-9.

Sadaie MR, Kalyanaraman VS, Mukopadhayaya R, Tschachler E, and Gallo RC, Wong-Staal F. 1992. Biological characterization of noninfectious HIV-1 particles lacking the envelope protein. *Virology* **187**(2): 604–611.

Sadler HA, Stenglein MD, Harris RS, Mansky LM. 2010. APOBEC3G contributes to HIV-1 variation through sublethal mutagenesis. *J Virol* **84**(14): 7396-404.

Sakai H, Shibata R, Sakuragi J, Sakuragi S, Kawamura M, Adachi A. 1993. Cell-dependent requirement of human immunodeficiency virus type 1 Vif protein for maturation of virus particles. *J Virol.* **67**(3): 1663-6.

Sandvig K and van Deurs B. 1996. Endocytosis, intracellular transport, and cytotoxic action of Shiga toxin and ricin. *Physiol Rev* **76**(4): 949-66.

Santa-Marta M, da Silva FA, Fonseca AM, Goncalves J. 2005. HIV-1 Vif can directly inhibit apolipoprotein B mRNA-editing enzyme catalytic polypeptide-like 3G-mediated cytidine deamination by using a single amino acid interaction and without protein degradation. *J Biol Chem* **280**(10): 8765-75.

Sasada A, Takaori-Kondo A, Shirakawa K, Kobayashi M, Abudu A, Hishizawa M, Imada K, Tanaka Y, Uchiyama T. 2005. APOBEC3G targets human T-cell leukemia virus type 1. *Retrovirology* **2**:32-42.

Sato Y, Probst HC, Tatsumi R, Ikeuchi Y, Neuberger MS, Rada C. 2010. Deficiency in APOBEC2 leads to a shift in muscle fiber type, diminished body mass, and myopathy. *J Biol Chem* **285**(10): 7111-8.

Sawyer SL, Emerman M, Malik HS. 2004. Ancient adaptive evolution of the primate antiviral DNA-editing enzyme APOBEC3G. *PLoS* **2**(9): E275.

Schäfer A, Bogerd HP, Cullen BR. 2004. Specific packaging of APOBEC3G into HIV-1 virions is mediated by the nucleocapsid domain of the gag polyprotein precursor. *Virology* **328**(2): 163-8.

Schröfelbauer B, Yu Q, Zeitlin SG, Landau NR. 2005. Human immunodeficiency virus type 1 Vpr induces the degradation of the UNG and SMUG uracil-DNA glycosylases. *J Virol* **79**(17): 10978-87.

Sheehy AM, Gaddis NC, Choi JD, Malim MH. 2002. Isolation of a human gene that inhibits HIV-1 infection and is suppressed by the viral Vif protein. *Nature* **418**(6898): 646-50.

Sheehy AM, Gaddis NC, Malim MH. 2003. The antiretroviral enzyme APOBEC3G is degraded by the proteasome in response to HIV-1 Vif. *Nat Med* **9**(11): 1404-7.

Siliciano JD and Siliciano RF. 2013. Recent trends in HIV-1 drug resistance. *Curr Opin Virol* **3**(5): 487-94.

Simon JH, Gaddis NC, Fouchier RA, Malim MH. 1998. Evidence for a newly discovered cellular anti-HIV-1 phenotype. *Nat Med* **4**(12): 1397-400.

Simon V, Zennou V, Murray D, Huang Y, Ho DD, Bieniasz PD. 2005. Natural variation in Vif: differential impact on APOBEC3G/3F and a potential role in HIV-1 diversification. *PLoS Pathog* **1**(1): e6.

Smith HC. APOBEC3G: a double agent in defense. 2011. *Trends Biochem Sci* **36**(5): 239-44.

Smith HC, Bennett RP, Kizilyer A, McDougall WM, Prohaska KM. 2012. Functions and regulation of the APOBEC family of proteins. *Semin Cell Dev Biol* **23**(3): 258-68.

Stein BS, Gowda SD, Lifson JD, Penhallow RC, Bensch KG, Engleman EG. 1987. pH-independent HIV entry into CD4-positive T cells via virus envelope fusion to the plasma membrane. *Cell* **49**(5): 659-68.

Stirpe F. 2004. Ribosome-inactivating proteins. *Toxicon* **44**(4): 371-83.

Stopak K, de Noronha C, Yonemoto W, Greene WC. 2003. HIV-1 Vif blocks the antiviral activity of APOBEC3G by impairing both its translation and intracellular stability. *Mol Cell* **12**(3): 591-601.

Strebel K, Daugherty D, Clouse K, Cohen D, Folks T, Martin MA. 1987. The HIV 'A' (sor) gene product is essential for virus infectivity. *Nature* **328**(6132): 728-30.

Svarovskaia ES, Xu H, Mbisa JL, Barr R, Gorelick RJ, Ono A, Freed EO, Hu WS, Pathak VK. 2004. Human apolipoprotein B mRNA-editing enzyme-catalytic polypeptide-like 3G (APOBEC3G) is incorporated into HIV-1 virions through interactions with viral and nonviral RNAs. *J Biol Chem* **279**(34): 35822-8.

Tazi J, Bakkour N, Marchand V, Ayadi L, Aboufirassi A, Branlant C. 2010. Alternative splicing: regulation of HIV-1 multiplication as a target for therapeutic action. *FEBS J* **277**(4): 867-76.

Teltow GJ, Irvin JD, Aron GM. 1983. Inhibition of herpes simplex virus DNA synthesis by pokeweed antiviral protein. *Antimicrob Agents Chemother* **23**(3): 390-6.

Teng B, Burant CF, Davidson NO. 1993. Molecular cloning of an apolipoprotein B messenger RNA editing protein. *Science* **260**(5115): 1816-9.

Thangavelu PU, Gupta V, Dixit NM. 2014. Estimating the fraction of progeny virions that must incorporate APOBEC3G for suppression of productive HIV-1 infection. *Virology* **449**:224-8.

Tor Y and Xie Y. 2009. New fluorescent nucleosides for real-time exploration of nucleic acids. *SPIE* DOI: 10.1117/2.1200912.002508.

Tumer NE, Hwang D, Bonness M. 1997. C-terminal deletion mutant of pokeweed antiviral protein inhibits viral infection but does not depurinate host ribosomes. *Proc Natl Acad Sci U S A* **94**(8): 3866-71.

Turelli P, Mangeat B, Jost S, Vianin S, Trono D. 2004. Inhibition of hepatitis B virus replication by APOBEC3G. *Science* **303**(5665): 1829.

Uckun FM, Bellomy K, O'Neill K, Messinger Y, Johnson T, Chen CL.1999. Toxicity, biological activity, and pharmacokinetics of TXU (anti-CD7)-pokeweed antiviral protein in chimpanzees and adult patients infected with human immunodeficiency virus. *J Pharmacol Exp Ther* **291**(3): 1301-7.

Ulenga NK, Sarr AD, Thakore-Meloni S, Sankalé JL, Eisen G, Kanki PJ. 2008. Relationship between human immunodeficiency type 1 infection and expression of human APOBEC3G and APOBEC3F. *J Infect Dis* **198**(4): 486-92.

van der Kuyl AC and Berkhout B. 2012. The biased nucleotide composition of the HIV genome: a constant factor in a highly variable virus. *Retrovirol* **9**:92.

Vartanian JP, Guétard D, Henry M, Wain-Hobson S. 2008. Evidence for editing of human papillomavirus DNA by APOBEC3 in benign and precancerous lesions. *Science* **320**(5873):230-3.

von Schwedler U, Song J, Aiken C, Trono D. 1993. Vif is crucial for human immunodeficiency virus type 1 proviral DNA synthesis in infected cells. *J Virol* **67**(8): 4945-55.

Vonica A, Rosa A, Arduini B, Brivanlou AH. 2010. APOBEC2, a selective inhibitor of TGFβ signaling, regulates left-right axis specification during early embryogenesis. *Dev Biol* **350**(1): 13-23.

Wang X, Ao Z, Chen L, Kobinger G, Peng J, Yao X. 2012. The cellular antiviral protein APOBEC3G interacts with HIV-1 reverse transcriptase and inhibits its function during viral replication. *J Virol* **86**(7): 3777-86.

Wedekind JE, Dance GS, Sowden MP, Smith HC. 2003. Messenger RNA editing in mammals: new members of the APOBEC family seeking roles in the family business. *Trends Genet.* **19**(4):207-16.

Wichroski MJ, Robb GB, and Rana TM. 2006. Human retroviral host restriction factors APOBEC3G and APOBEC3F localize to mRNA processing bodies. *PLoS Pathog* **2**(5): e41.

Wood N, Bhattacharya T, Keele BF, Giorgi E, Liu M, Gaschen B, Daniels M, Ferrari G, Haynes BF, McMichael A, Shaw GM, Hahn BH, Korber B, Seoighe C. 2009. HIV evolution in early infection: selection pressures, patterns of insertion and deletion, and the impact of APOBEC. *PLoS Pathog* **5**(5):e1000414

Xu H, Chertova E, Chen J, Ott DE, Roser JD, Hu WS, Pathak VK. 2007. Stoichiometry of the antiviral protein APOBEC3G in HIV-1 virions. *Virology* **360**(2): 247-56.

Yang B, Chen K, Zhang C, Huang S, Zhang H. 2007. Virion-associated uracil DNA glycosylase-2 and apurinic/apyrimidinic endonuclease are involved in the degradation of APOBEC3G-edited nascent HIV-1 DNA. *J Biol Chem* **282**(16): 11667-75.

Yu X, Yu Y, Liu B, Luo K, Kong W, Mao P, Yu XF. 2003. Induction of APOBEC3G ubiquitination and degradation by an HIV-1 Vif-Cul5-SCF complex. *Science* **302**(5647): 1056-60.

Yu Q, König R, Pillai S, Chiles K, Kearney M, Palmer S, Richman D, Coffin JM, Landau NR. 2004a. Single-strand specificity of APOBEC3G accounts for minus-strand deamination of the HIV genome. *Nat Struct Mol Biol* **11**(5): 435-42.

Yu Y, Xiao Z, Ehrlich ES, Yu X, Yu XF. 2004b. Selective assembly of HIV-1 Vif-Cul5-ElonginB-ElonginC E3 ubiquitin ligase complex through a novel SOCS box and upstream cysteines. *Genes Dev* **18**(23): 2867-72.

Zarling JM, Moran PA, Haffar O, Sias J, Richman DD, Spina CA, Myers DE, Kuebelbeck V, Ledbetter JA, Uckun FM. 1990. Inhibition of HIV replication by pokeweed antiviral protein targeted to CD4+ cells by monoclonal antibodies. *Nature* **347**(6288): 92-5.

Zennou V, Perez-Caballero D, Göttlinger H, Bieniasz PD. 2004. APOBEC3G incorporation into human immunodeficiency virus type 1 particles. *J Virol* **78**(21):12058-61.

Zhabokritsky A, Mansouri S, Hudak KA. 2014. Pokeweed antiviral protein alters splicing of HIV-1 RNAs, resulting in reduced virus production. *RNA* **20**(8): 1238-47.

Zhang G, Zapp ML, Yan G, Green MR. 1996. Localization of HIV-1 RNA in mammalian nuclei. *J Cell Bio* **135**(1): 9-18.

Zhang H, Yang B, Pomerantz RJ, Zhang C, Arunachalam SC, Gao L. 2003. The cytidine deaminase CEM15 induces hypermutation in newly synthesized HIV-1 DNA. *Nature* **424**(6944): 94-8.

Zhang W, Du J, Evans SL, Yu Y, Yu XF. 2011. T-cell differentiation factor CBF-β regulates HIV-1 Vif-mediated evasion of host restriction. *Nature* **481**(7381): 376-9.

Zielonka J, Bravo IG, Marino D, Conrad E, Perković M, Battenberg M, Cichutek K, Münk C. 2009. Restriction of equine infectious anemia virus by equine APOBEC3 cytidine deaminases. *J Virol* ***83***(15): 7547-59.

Zuo T, Liu D, Lv W, Wang X, Wang J, Lv M, Huang W, Wu J, Zhang H, Jin H, Zhang L, Kong W, Yu X. 2012. Small-molecule inhibition of human immunodeficiency virus type 1 replication by targeting the interaction between Vif and ElonginC. *J Virol* **86**(10): 5497-507.